

Japanese Finger Sleeves

BME 200/300

University of Wisconsin-Madison

Department of Biomedical Engineering

10/07/2025

Team Members:

Ilia Mikhailenko (Co-Team Leader)

Nathan Hansen (Co-Team Leader)

Ben Willihnganz (BWIG)

Mariamawit Tefera (Team Communicator)

Nathan Klauck (BSAC)

Sam Dudek (BPAG)

Client: Mr. Pape Samb

Advisor: Dr. Justin Williams, BME Department

ABSTRACT

Hand traction is essential in orthopedic and surgical procedures to maintain wrist alignment and joint stability during forearm procedures and casting. At Idrissa Poye Hospital in Senegal, the loss of their previous traction device left clinicians without a reliable method to stabilize the hand, forcing them to depend on manual traction or improvised setups. These workarounds reduce accuracy, increase clinician workload, and introduce safety risks for patients. Existing hand-traction technologies are often expensive, immobile, or incompatible with low-resource settings, underscoring the need for a durable, adjustable, and sterilizable alternative. This design project developed a digital traction device designed specifically to address these limitations by providing consistent, comfortable, and easily adjustable traction while minimizing physical strain on both patients and medical staff. The device integrates an adjustable mechanical body, “one size fits all” finger sleeves, and materials suitable for repeated sterilization. Through Finite Element Analysis, the mechanical body of the device was confirmed to withstand clinically relevant traction forces. The ballistic nylon finger sleeves maintained structural integrity under sterilization conditions which was confirmed in Autoclave Tensile Testing. Lastly, Slippage Displacement Testing proved the device securely holds the weight of the hand and arm with minimal displacement during simulated use. Overall, results indicate that the proposed device provides a safe, effective, and sustainable solution for hand stabilization in low-resource clinical environments, with the potential to reduce clinician fatigue, improve surgical precision, and enhance patient outcomes.

TABLE OF CONTENTS

ABSTRACT	2
1 INTRODUCTION	5
1.1 Motivation	5
1.2 Existing Devices & Current Methods	5
1.3 Problem Statement	7
2 BACKGROUND	9
2.1 Biology and Physiology	9
2.2 Relevant Research	10
2.3 Client Information	10
2.4 Product Design Specification	11
3 PRELIMINARY DESIGNS	12
3.1 Mechanical Design 1 - Standing Platform	12
3.2 Mechanical Design 2 - Bed Clamp & Restraint	13
3.3 Mechanical Design 3 - Extension Brace	14
3.4 Finger Sleeve Design 1 - Nylon Sleeve	15
3.5 Finger Sleeve Design 2 - Hand Brace	16
3.6 Finger Sleeve Design 3 - Buckle and Strap	17
4 PRELIMINARY DESIGN EVALUATION	18
4.1 Design Matrix	18
4.2 Proposed Final Design	21
5 FABRICATION	23
5.1 Materials	23
5.2 Methods	23
5.3 Final Prototype	25
6 TESTING & RESULTS	27
7 DISCUSSION	32
8 CONCLUSION	34
9 REFERENCES	35
10 APPENDIX	37
10.1 Product Design Specification	37
10.2 Mechanical Stand Fabrication Protocol	46
10.3 Mounting Plate CAD Drawing	48
10.4 In-place Mounting Plate Stopper CAD Drawing	49
10.5 Finger Sleeve Fabrication Protocol	49
10.6 Finger Sleeve D-Ring CAD Drawing	52
10.7 Finite Element Analysis Testing Protocol	52

10.8 Autoclaved Tensile Testing Protocol	53
10.9 Autoclaved Tensile Testing Raw MTS Data	54
10.10 Autoclaved Tensile Testing MATLAB Code	55
10.11 Dog Bone CAD Drawing	62
10.12 Slippage Testing Protocol	62
10.13 Slippage Testing Raw Data	63
10.14 Stitched Tensile Testing Protocol	64
10.15 Stitched Tensile Testing Raw MTS Data	65
10.16 Stitched Tensile Testing MATLAB Code	66
10.17 Expense Report	69

1 INTRODUCTION

1.1 Motivation

Fractures of the distal upper extremity are highly common in the orthopedic world, accounting for approximately 17.5% of all fractures [1]. An essential instrument used to repair these fractures is a digital traction device, which applies a controlled longitudinal force to the finger and forearm to facilitate proper alignment and fixation. An effective traction device achieves this by sustaining a load on the upper extremity while also relaxing the surrounding musculature for the entirety of surgical or rehabilitative procedures. The maintenance of a steady static load on the finger and forearm is crucial to not only ensure correct fracture realignment, but also to prevent unintended movement throughout the procedure [2]. Beyond just being functionally sound, a well-designed traction device also maintains patient comfort by minimizing soft tissue strain and unnecessary joint distraction.

Traction has long been used in the medical industry, but its use has decreased over time and the quality of traction devices has declined as a result [2]. Surgeries that utilize inadequate traction devices can lead to stiffness, surgical complications, and even loss of motor function in affected regions of the body [3].

In many low- and middle-income healthcare settings, traction often has to be performed manually. This method of traction is suboptimal because it requires hospital workers to physically maintain the tension of the patient's arm for the entire surgery. This can often lead to physician fatigue and flawed outcomes. Although commercial traction systems exist, their intricate designs and high price points make it difficult for hospitals like the client's to supply and manage these devices. This emphasizes a common problem for resource-constrained regions. They often lack equipment because of issues with accessibility and sustainability within the hospital. The client stated that "[they] are fully redundant with foreign suppliers" [4]. Overall, the objective of this project is to create a versatile and locally manufacturable system that can work in a sterile and non-sterile environment. This will address the clients initial needs while also functioning as a path towards more equitable access to healthcare.

1.2 Existing Devices & Current Methods

The field of orthopedic traction systems includes both simple gravity-based finger traps and more complex mechanical stabilization frames. These devices vary in their level of precision, comfort, and adjustability. Although they perform well in certain contexts, none fully meets the client's current needs for a lightweight, sleeve-based digital traction system.

The Reison Hand Fixation Device (Reison Medical, Part No. 10-394) provides rigid stabilization of the hand and forearm during surgery using stainless steel and polycarbonate components. The device is adjustable to accommodate different hand sizes and offers strong

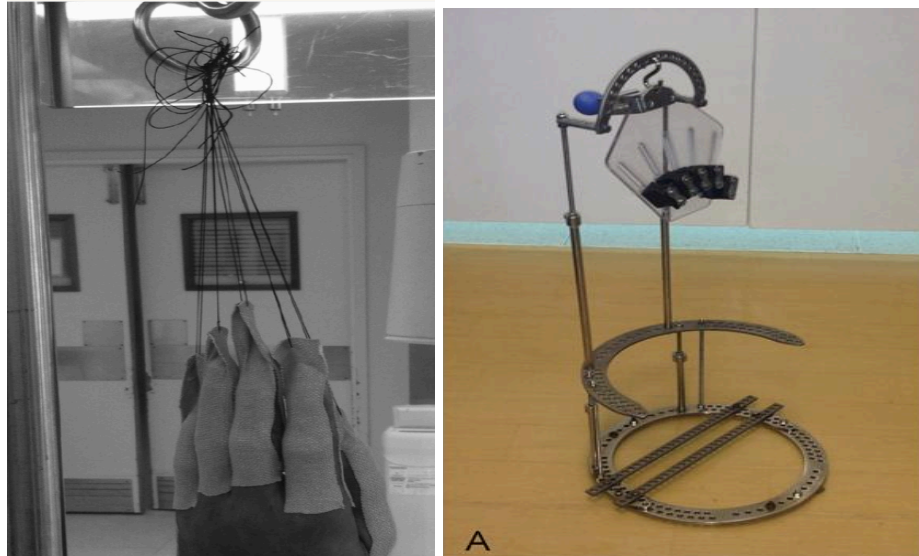
positional stability during fracture repair or fixation procedures, as shown in Figure 1 [5]. Despite its stability, it is heavy and static, lacking individual finger mobility and ergonomic flexibility. These limitations make it less ideal for longer procedures where patient comfort and clinician control are critical.



Figure 1: Reison Hand traction [5]

The Chinese Finger Trap System is a traditional device for wrist and forearm traction. It suspends the patient's hand using woven finger sleeves, allowing gravity to apply continuous traction. A readily available alternative described by Akhtar et al. (2013) demonstrates how clinicians sometimes substitute tape for the woven traps when the original device is unavailable [6]. Although effective in generating traction, this system depends entirely on gravity, offers limited adjustability, and lacks built-in feedback or sensing capabilities. Moreover, availability can be inconsistent, particularly in resource-limited or after-hours clinical settings, making it an unreliable option for the client's needs. Figure 2 illustrates a standard finger trap setup [6, 7].

The third device analyzed was the Handmade Traction Wrist Tower, also referred to as the Hook and Trumpf Hand Holder [7]. This system consists of a metal base with an S-shaped hook and adjustable rods designed to create controlled traction across the fingers and wrist. Foam padding is used to protect soft tissue at points of contact, but the overall design is large and metal-based. While it provides adjustability, its weight and bulk limit ergonomic efficiency and portability. The device is shown in Figure 2 [6, 7].



Figures 2: Chinese finger traps (left) and Hook-and-Trumpf (right) [6, 7]

The designs presented above are all functional and commercially available but lack critical features needed for the client's environment. However, they are high-cost systems that are difficult for the client to procure reliably and lack the portability needed to move easily between treatment areas throughout the hospital. Section 3.1 (Design 1) further discusses how these limitations guided the team's development of an improved, sleeve-based digital traction device capable of improving upon the weaker functionality of the client's current device.

1.3 Problem Statement

The client's medical facility, Idrissa Pouye Hospital, is a resource-constrained healthcare center in the metropolitan area of Dakar, Senegal. The hospital formerly made use of Japanese finger traps for digital traction; however, these systems were either lost or experienced deterioration due to repeated use. With the limited supply of medical devices in the Dakar region as well as Idrissa Pouye Hospital's restricted budget, digital traction devices are currently not being repurchased by the facility. Instead, the hospital staff use manual traction to stabilize the wrist and forearm during casting, wrist arthroscopies, and other procedures. However, manual traction is suboptimal because it is imprecise for the doctor and often uncomfortable or painful for the patient. This leads to less successful surgeries as well as a longer patient recovery time. Manual traction also requires multiple clinicians to sustain traction and provide treatment, which is an inefficient use of personnel in a hospital that treats 50,000 orthopedic patients per year [4].

Due to the high patient volume and the frequent handling of traction devices, there is a significant risk that any given device will eventually be lost, misplaced, or damaged beyond repair. As a result, the client is not only seeking a low-cost traction system, but also one that can be reliably manufactured on demand using materials and fabrication methods available in or near

Dakar. This would allow Idrissa Pouye Hospital to replace broken or missing devices quickly and maintain an adequate supply without depending on expensive, slow, or uncertain supplier procurement.

The commercial traction devices outlined in Section 1.2 are effective, but their high cost and complicated nature make them unsuitable for local production in the client's low-resource setting. Furthermore, the models currently available on the market cannot be used in both the non-sterile plaster casting room, as well as the sterile operating room. This is most often due to either a lack of mobility, restricted access to the forearm, or limited reusability of the device.

The objective of this project is to create a digital traction device using finger traps that precisely pulls the patient's hand, wrist, and forearm into a comfortable, neutral position while holding a stable static load. To be feasible for Idrissa Pouye Hospital, the device must be portable and usable in both the plaster casting room and the operating room. This requires a compact and mobile device that can be transported easily between spaces, provides unobstructed access to the forearm for casting and arthroscopy, and tolerates routine sterilization without loss of function. In addition, the design must be simple enough to fabricate, assemble, and repair using materials and processes available in or near Dakar so that the hospital can maintain a reliable inventory even as individual devices are lost or damaged over time.

2 BACKGROUND

2.1 Biology and Physiology

To grasp the impact of digital traction systems, it is essential to understand the anatomy and physiology of the treatment area. As a whole, the wrist and forearm provide mobility and structural support for the hand. The forearm consists of two long bones, the radius and the ulna. These bones allow for support and flexibility during pronation and supination, which are common movements of the forearm. The distal end of the radius connects to the carpal bones through the radiocarpal joint. This joint enables flexion and extension of the wrist, which is critical for many everyday human activities [4]. The carpus is the collection of eight small bones held together by stabilizing ligaments. These bones are often susceptible to fractures when subjected to heavy loads and rotational movements as a result of their small size relative to other hand bones, which can be observed in Figure 3 [1]. The carpal tunnel also encloses many tendons and the median nerve.

This compact and intricate collection of bones, ligaments, and tendons makes it crucial to be highly precise when operating on this region of the body. This means that the digital traction device must maintain the hand in a neutral position, neither flexed nor extended, throughout the entirety of surgical and casting procedures to promote effective realignment of the hand bones by reducing internal stress and protecting soft tissue [8].

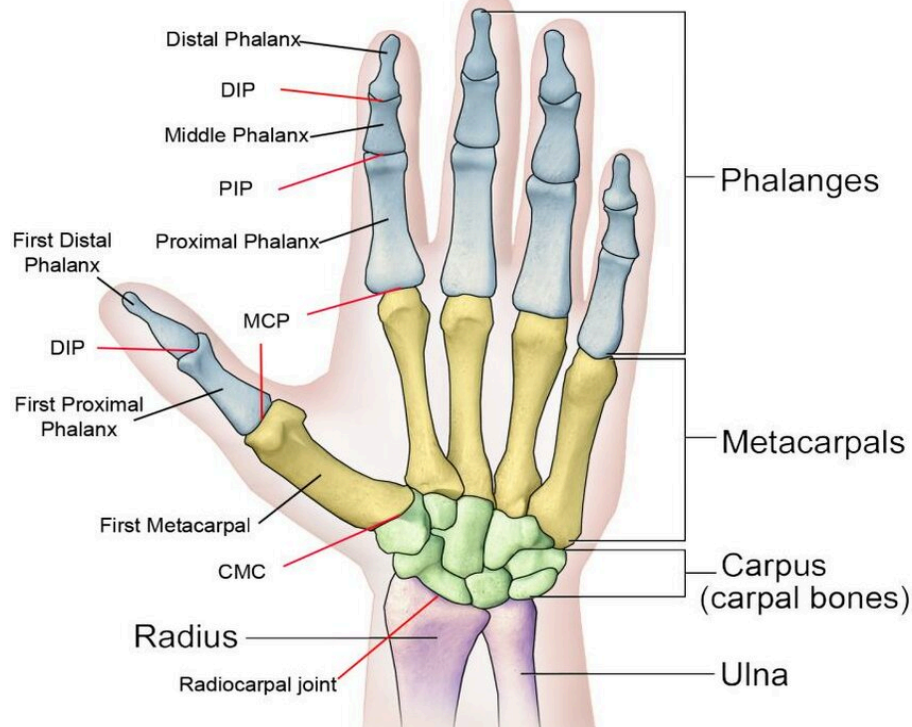


Figure 3: Anatomical drawing of the hand, wrist, and forearm [1]

As stated earlier, distal radius fractures are very common in the orthopedic setting [1]. In procedures performed to treat these fractures, digital traction can serve as a diagnostic and therapeutic tool. It aligns small bone fragments and can prevent neurovascular compromise, leading to better patient outcomes [2]. Therefore, maintaining consistent traction with a neutral wrist and forearm position is critical to performing a successful surgery and preventing future complications for the patient.

2.2 Relevant Research

Developing a digital traction device that needs to be locally reproducible and adaptable enough to be used both in surgery and casting requires knowledge in many areas, including logistical, regulatory, and biological fields. Biomechanical research on the forces applied to the wrist during use of the device is an area of important note. This research allows for knowledge of safe thresholds, and methodologies of keeping the wrist in a neutral position for long periods of time. Articles that outline the process of traction devices often range on the scale of the whole body and across numerous hospitals and regions of the world. Further, it is also necessary to complete anatomical and biological research, to recognize what parts of the body are being acted on, and their specific physiology. This will inform proper alignment in regards to positioning of the wrist and forearm. This information, including safe force thresholds and anatomical considerations, is provided in greater detail in Appendix 10.1 (Product Design Specification).

On the more logistical side of things, research must be done on the materials. This device comes into contact with the human, so materials must be medical grade, non-allergenic, and sterilizable [9]. Further, both aspects of the design need to endure sterilization without degrading. Lastly, an extensive amount of research needs to be done on the regulatory standards regarding medical devices. Relevant standards were studied such as ISO 13485:2016 for quality management systems, ISO 10993-1:2018 for biocompatibility testing, ISO 14971:2019 for risk management, and more. On top of that, research was conducted to learn more about medical device quality system regulation in the U.S. such as FDA 21 CFR Part 820, even if this project is for Senegal. All of this is to make sure the device aligns with the recognized rules for a medical device such as this one.

2.3 Client Information

Mr. Pape Samb is the founder and executive director of Jamerek, a non-profit organization based in Sun Prairie. He also serves on the board of the Sun Prairie Media Center and is a community TV and radio producer [10]. Dr. Mohamed Soumah is a doctor at Idrissa Pouye Hospital in Senegal, a medical facility that treats approximately 50,000 orthopedic fractures on an annual basis [4].

2.4 Product Design Specification

The product design specification defines the functional, safety, and performance requirements of the digital traction device using Japanese finger sleeves. The goal of the design is to provide a stable and controlled method for hand positioning during orthopedic and surgical procedures, while maintaining patient comfort and clinical efficiency.

The device functions as a digital traction system that uses Japanese finger sleeves to achieve precise stabilization of the hand and wrist. It must be capable of supporting the patient's hand for approximately fifty minutes during fracture casting or surgery without slippage or loss of tension. To meet these requirements, each sleeve must support a consistent traction force in the range of 22 to 44 N per finger, ensuring even load distribution and stability throughout the procedure.

In terms of safety and materials, the design must use latex-free materials to prevent allergic reactions, preferably non-metallic components, and allow for use in imaging environments. The sleeve system must also minimize compression to avoid interference with circulation or nerves, while maintaining a sufficient grip to hold each finger securely. The materials must be biocompatible and sterilizable, capable of withstanding repeated autoclave or chemical sterilization without degradation or loss of elasticity.

To accommodate a variety of hand sizes, the traction sleeves should feature adjustable or multiple size options that can comfortably fit various finger diameters. The device must provide a high-friction grip for stability and dexterity, while allowing natural finger flexion and extension to ensure tendons glide smoothly during minor patient movements. Regarding service life, the finger sleeves must reliably perform at least 500 full uses over their service lifetime, with each use lasting 50 minutes under load. The sleeves should maintain full function for at least two years, with a stock of 36 sets accounting for daily use. Elastic and sensor components should endure up to 100,000 loading cycles. Device components must retain functionality for at least three years when stored at 10–30 °C, below 70% relative humidity, and protected from direct UV light. The operating environment includes standard surgical conditions (20–24 °C, 20–60% relative humidity), with surfaces resistant to blood, saline, antiseptics, and disinfectants.

Together, these specifications establish the quantitative and qualitative standards for prototype development and evaluation. The full PDS, including supporting references and regulatory standards, is provided in Appendix 10.1 (Product Design Specification).

3 PRELIMINARY DESIGNS

The design was divided into two components, the mechanical structure and hand attachment method. This allowed for the development of three designs for each separately, and a more focused evaluation of each component's function without limiting potential combinations.

3.1 Mechanical Design 1 - Standing Platform

The first mechanical design features a free standing traction platform intended for use during rehabilitation or preoperative preparation, seen in Figure 4. The device consists of a vertical base pole with wide set locking wheels for stability and mobility. The base accepts a removable extender pole that allows for height adjustment and a curved arm on top of the extender pole that rotates 360° to accommodate patient positioning. The curved upper arm also supports individualized tension cables that connect to finger loops, which are attachment points for the finger sleeves that provide controlled traction for each finger. A force control box, located along the main support pole, would regulate and display finger specific traction forces. The arm assembly can also be detached and inserted into a clamp down platform different from the wheeled base shown. This enhances its versatility and cost effectiveness by allowing both stationary and mobile configurations.

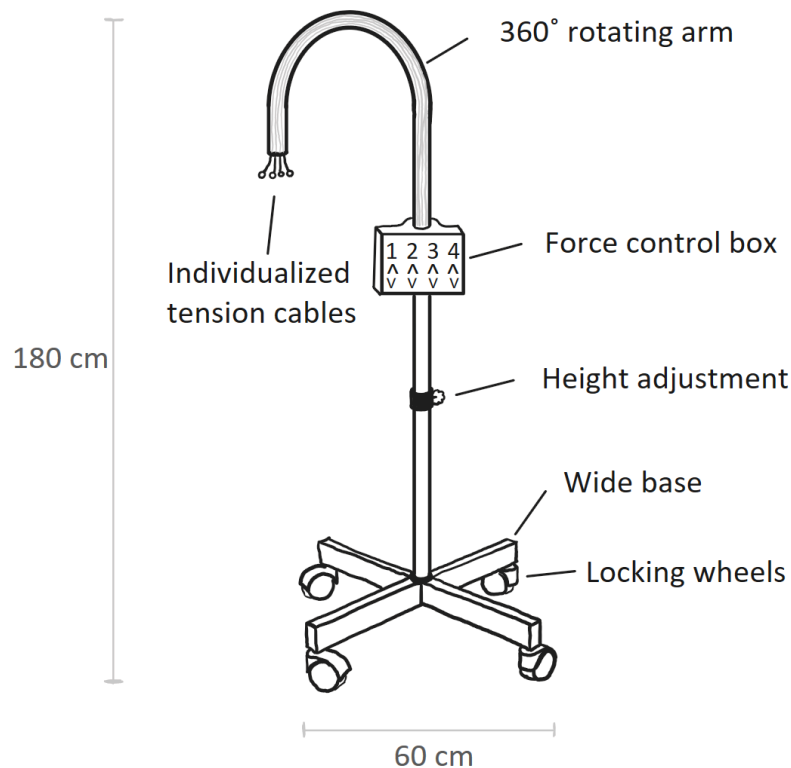


Figure 4: Stranding structure on wheeled base design

3.2 Mechanical Design 2 - Bed Clamp & Restraint

The second mechanical design features a sleek structure that mounts directly to the frame of a hospital bed, as seen in Figure 5. The base of the device is secured using a heavy-duty clamp that mechanically interacts with the shape of the bed frame, which locks the entire system in place, preventing movement during use. A circular, vertical mounting post extends upward, serving as an attachment point for other components. All attachments connect to the post with an adjustable stand clamp that uses a hand tightened set screw, allowing each component to be moved freely up and down and rotated 360° around the post to accommodate different arm lengths and sizes. One component is a bicep restraint arm, positioned lower on the post. This arm features a curved, ergonomic plate that presses down on the top of the bicep, stabilizing the arm by blocking upward movement under tension. An adjustable upper arm is attached higher on the post, which secures the device that applies the tension force to the lower arm. This arm has a plate with five holes in it, for finger sleeve attachment, to apply an even amount of force to each finger.

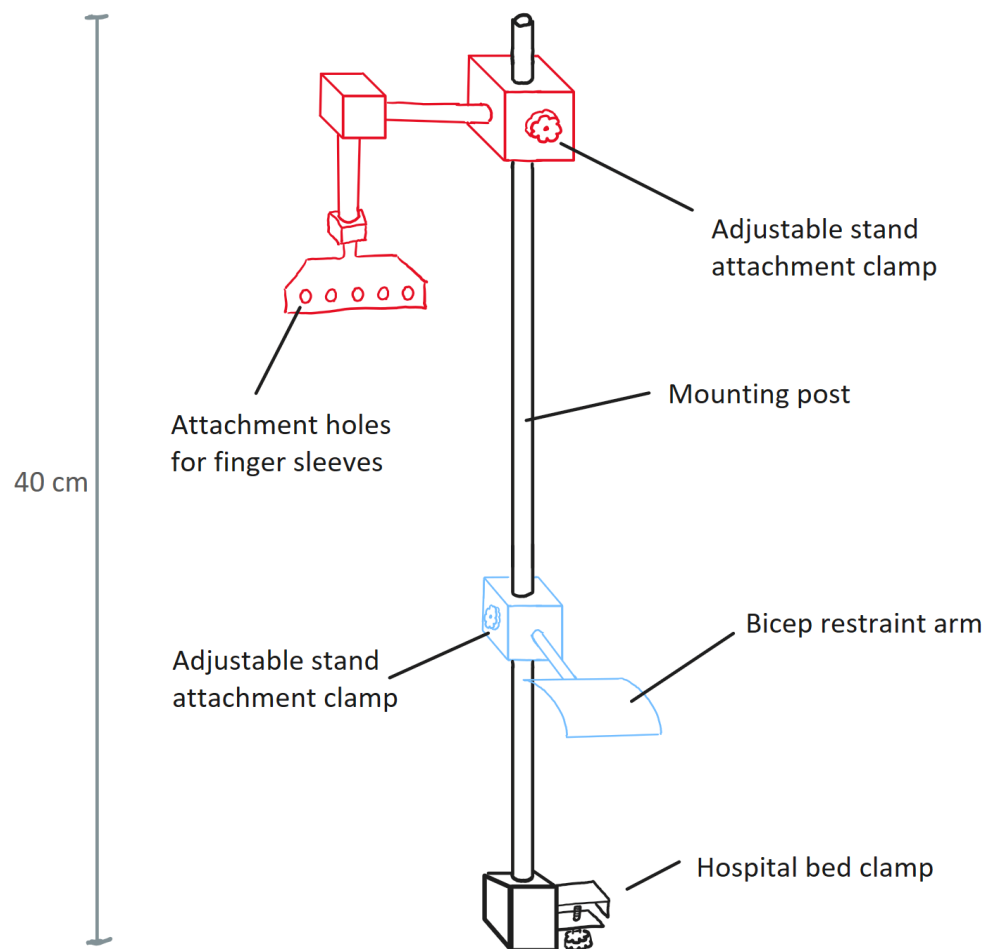


Figure 5: Bed clamp with restrain arm design

3.3 Mechanical Design 3 - Extension Brace

The third mechanical design is an arm and hand orthosis, used to support and position a patient's whole arm below the shoulder, seen in Figure 6. The upper arm and proximal forearm are secured by multiple Velcro straps over contoured arm padding, ensuring a secure and comfortable fit. A locking elbow hinge connects the upper arm and forearm components, allowing for adjustment and fixation of the elbow angle. Extending distally from the hinge is a rigid extension bar, which leads to the hand portion of the orthosis. The elbow hinge contains a mechanism which allows for the extension bar to slide and be fixed at precise points. This movement adjusts the distance between the elbow and hand, applying tension to the lower arm. The hand is stabilized by a hand strap positioned across the palm and individual fingers are secured by several finger straps, however this is subject to change depending on the determined finger sleeve design.

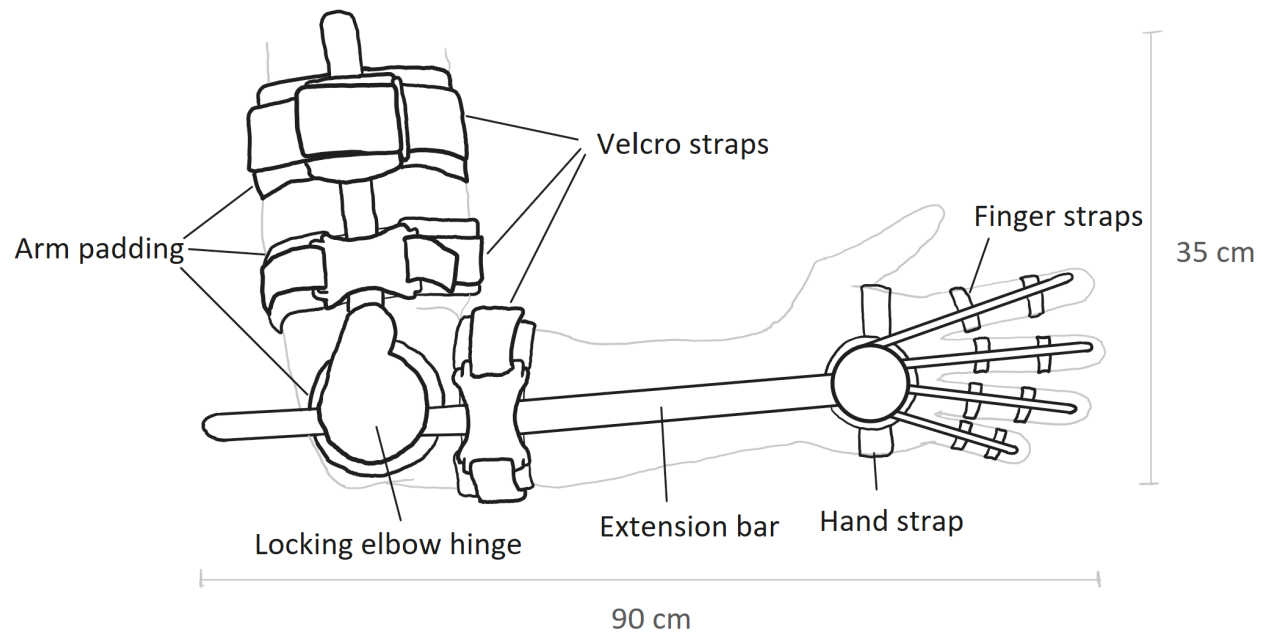


Figure 6: Extension brace design

3.4 Finger Sleeve Design 1 - Nylon Sleeve

The first finger sleeve design is most similar to the leading designs on the market. Its primary feature is a braided nylon mesh that surrounds the entire finger and, when stretched, grips the finger allowing tension to be applied to the digits, as seen in Figure 7. The rubber stopper, displayed in the image below, prevents the eye hook from pulling through the mesh of the sleeve. The eye hook is attached to the mechanical portion of the device through a connection method. This eye hook can then be pulled on, tightening and lengthening the braid of the nylon material, which in turn compresses around the finger providing the traction for the design. The final component of this design is the synching rubber band placed at the bottom of the sleeve. This rubber band aids the applicator, as it allows the finger sleeve to connect with the finger before the tension force is applied. This design allows for ideal control over each finger, but in order for the correct compressive forces to be applied, would also require select size to be produced to fit all finger types.

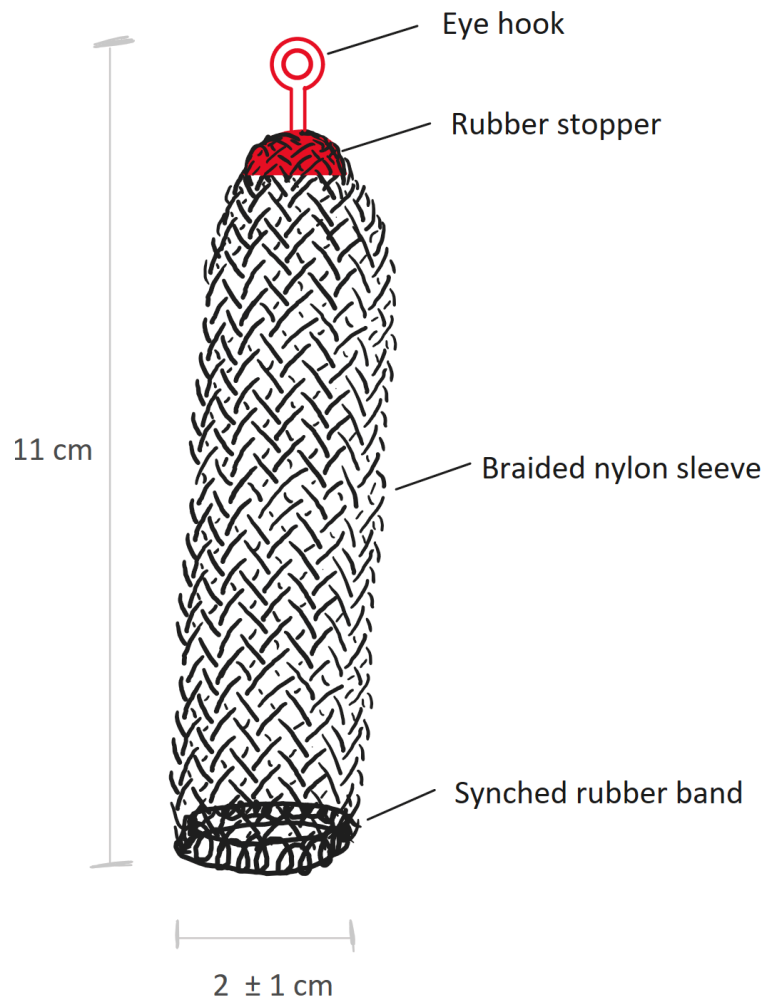


Figure 7: Braided Nylon mesh sleeve design

3.5 Finger Sleeve Design 2 - Hand Brace

The second finger sleeve design is an immobilization device, seen in Figure 8. The device consists of a rigid backed plate that helps in immobilizing the hand itself. The rigid backed plate is then surrounded by a foam material that will aid in the overall comfort of the design for the patients. Flexible finger tabs are inserted into the end of the finger structures of the brace that are able to bend over the palm side of the finger to prevent overall finger movements. The hand tabs, as labeled below, function similarly to the finger tabs, but instead of being inserted at the end of the fingers, they erect from the radial and ulnar sides of the hand, immobilizing the lower hand. This hand brace device would be connected to the mechanical frames in a unique way as there is no built-in connection to the frame, which is a particular drawback to this design. This device would be a universal fit for all finger lengths and hand sizes. This could be accounted for with long finger tabs that can aid in the immobilization of the digits and the wrist joint.

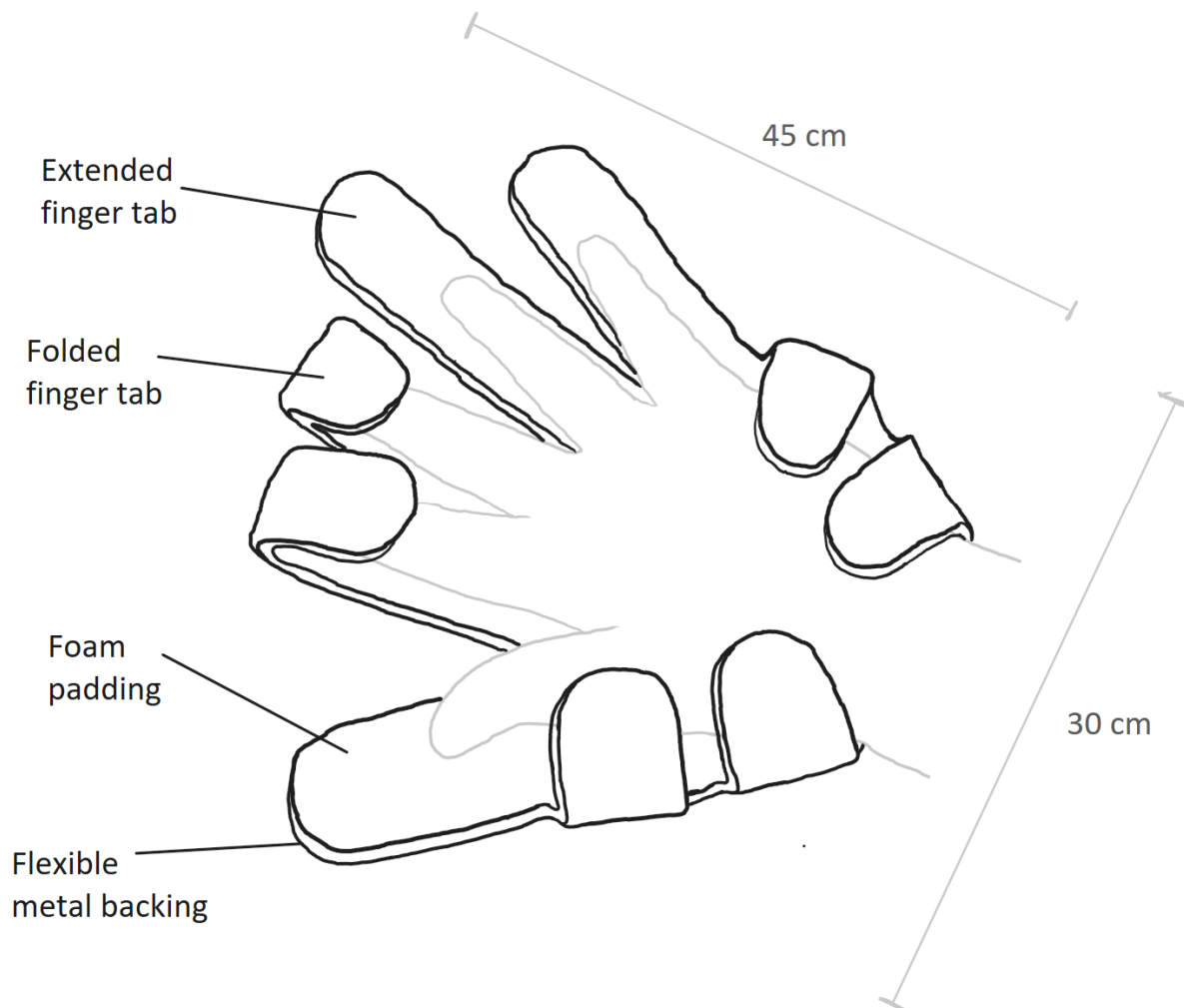


Figure 8: Universal hand brace design

3.6 Finger Sleeve Design 3 - Buckle and Strap

The third design consists of a nylon strip that is tightened around the finger using 2 separate velcro buckles that are fastened down by straps, seen in Figure 9. For the connection to the mechanical part of the design, a D ring is placed at the end of the device to allow for connection to the frame. Overall this device is functionally similar to a standard finger splint, without the rigidity. The flexible nylon finger sleeve allows for slight freedom of movement, creating versatility for the surgeon. The blue strap in Figure 9 can slide up and down the length of the sleeve to be secured under the knuckle, aiding in immobilization and traction in the digits. The bottom strap can open as wide as 3 centimeters in order to fit any finger girths. Lengths of the nylon straps will be long enough to ensure any size finger can fit into the design and the buckles will ensure traction for every finger girth.

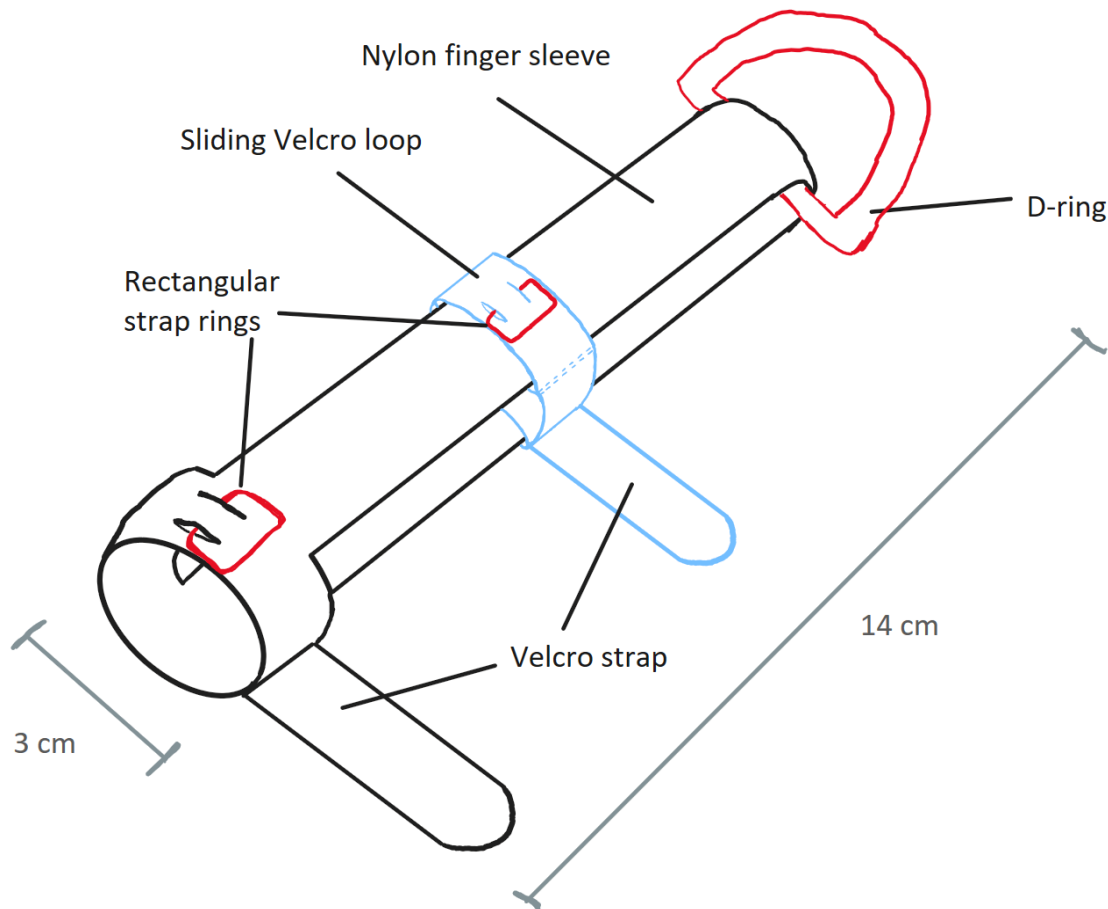


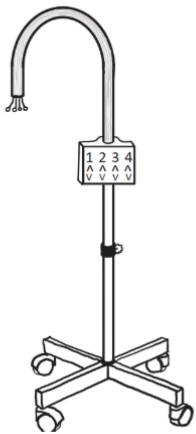
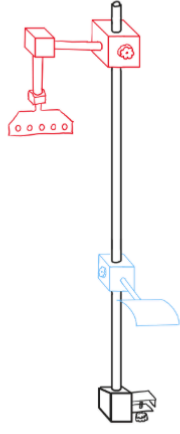
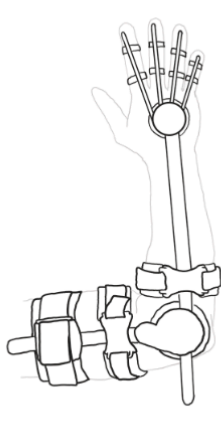
Figure 9: Buckle and Velcro strap sleeve design

4 PRELIMINARY DESIGN EVALUATION

4.1 Design Matrix

Table 1 shows the project scope design matrix for the mechanical portion of the design, which has the categorical rankings explained below.

Table 1: A design matrix created to rank the three preliminary designs for the mechanical portion of the digital traction device. Each category is rated by importance and is used to determine an overall score for each design.

Design Criteria	Standing Platform		Bed Clamp & Restraint		Extension Brace	
						
Ease of use (25)	5/5	25	4/5	20	3/5	15
Cost (20)	4/5	16	5/5	20	2/5	8
Reusability (15)	4/5	12	5/5	15	2/5	8
Safety (15)	3/5	9	4/5	12	5/5	15
Ease of Fabrication (15)	4/5	12	5/5	15	2/5	6
Versatility (10)	4/5	8	3/5	6	2/5	4
Total (100)	82/100		88/100		56/100	

Reasonings for Scores

Ease of Use

Ease of use is defined as the device's ability to assist doctors and hospital staff during various procedures while also smoothly integrating into existing hospital practices. This is weighted the highest because the primary goal of the device is to reduce the effort and manual labor required of the medical team in their day-to-day operations.

Cost

Cost is weighted the second-highest because the client's goal is to manufacture the device in Senegal within the hospital's limited budget. Keeping the cost of each traction device low makes it more affordable and accessible, which could significantly improve the hospital's ability to treat its orthopedic patient population.

Reusability

Reusability is defined as the device's ability to withstand the repeated sterilization required in the operating room without losing the qualities necessary for it to function properly. This is weighted highly because it reflects the device's longevity and the number of cases it can be used for before needing replacement.

Safety

Safety is defined as how effectively the device minimizes the risk of harm to patients and hospital staff. This is weighted fairly high because a device that risks harming those around it runs directly counter to a hospital's mission of improving the health of the people it serves.

Ease of Fabrication


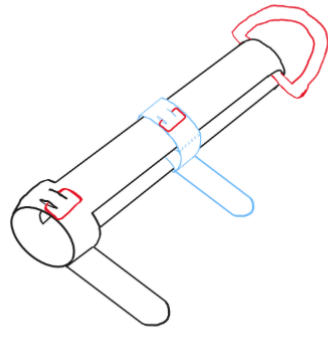

Ease of fabrication is defined as the device's ability to be manufactured on site in Senegal. It depends largely on the simplicity of the design, the ease of producing each component, and the difficulty of assembling them. This is weighted lower because, while still important, it is influenced more by material selection than by the methods chosen.

Versatility

Versatility defines the ability of the digital traction device to be used in a wide range of hospital settings, including the operating room as well as the rehabilitative clinic. Although it is not as important as the device's functionality, adaptability still warrants consideration as the device being effective in different medical contexts is helpful for both users and patients.

Table 2 shows the project scope design matrix for the sleeve portion of the design, which has the categorical rankings explained below.

Table 2: A design matrix created that was used to rank the three preliminary designs for the sleeve portion of the digital traction device. Each category is rated by importance and is used to determine an overall score for each design.

Design Criteria	Nylon Sleeve		Buckle and Strap		Hand Brace	
						
Safety (25)	5/5	25	4/5	20	2/5	10
Ease of Fabrication (20)	2/5	8	5/5	20	4/5	16
Cost (20)	3/5	12	5/5	20	2/5	8
Ease of Use (15)	5/5	15	4/5	12	3/5	9
Comfort (10)	4/5	8	3/5	6	5/5	10
Reusability (10)	2/5	4	4/5	8	2/5	4
Total (100)	72/100		86/100		57/100	

Reasonings for Scores

Safety

Safety is defined as to how effectively the design prevents risk to patients health, in this case specifically due to loss of circulation or slippage from device. This is weighted the highest as patient safety is the highest priority in a healthcare setting.

Ease of Fabrication

Ease of fabrication refers to the time and skill necessary to assemble a finger sleeve. This was weighted second highest as the client needs an efficient design to be manufactured in Senegal, and further multiple of the sleeve is required for each device.

Cost

Cost refers to the cost of materials and tools to construct each sleeve. This was weighted second highest as well due to the importance of a cost effective design to be manufactured in Senegal especially with each design requiring multiple sleeves.

Ease of Use

Ease of use refers to how easy the device is to apply to a patient's hand and whether the design gets in the way of any operations. This was weighted next highest as the client wants the design to not impede the work of clinicians within the healthcare setting.

Comfort

Comfort refers to the comfort of the device to the patient both during short and long term use. This was weighted one of the lowest as despite the importance of making a comfortable design for the patient, it's not as important as designing a safe and easily manufacturable device for the design criteria

Reusability

Reusability refers to the ease of cleaning of the device and whether its design allows for reuse. This was rated the lowest as although its valuable to have a device you can use multiple times, due to the necessity of an easily fabricated design quantity should not be a problem

4.2 Proposed Final Design

The proposed final design for the mechanical and sleeve portion of the device is a hybridized bed clamp and restraint with a detachable wheel base, seen in Figure 10, that utilizes a buckle and strap design finger sleeve. The decision to go with a hybridized design was based on the close scoring on the mechanical design matrix. Particularly, this new design was made based on the bed clamp and restraints design's ease of use, cost, and reusability. The ease of use of this device comes from its ability to be easily clamped onto a typical patient's bed and the simplistic attachment method. Further the cost of this device sets it apart due to its simplistic design requiring very few intricate parts to manage the device. Similarly the simplicity of the design allows for the device to be more easily cleaned and designed out of parts more resistant to cleaning techniques, making it more reusable. This device struggled in terms of its versatility, but

the standing platform excelled in this category due to its wheel base, allowing for increased transfer mobility and positioning. Therefore, a simple addition of a detachable wheel base was made to the bed clamp and restraint design. The decision to go with a buckle and strap design is due to the device's ease of fabrication and cost as well as a good safety. The device's simplistic design and cheap design material because this design allows for the use of a material within the \$50 budget. This allows the device to be both easily fabricated and low cost, allowing for large scale production to accommodate the needs in Senegal. Further the device meets safety requirements due to the nature of its two contact point design. This design struggled in terms of comfort due to the two strap design. However, after taking into consideration all the aspects in the decision matrix, this was the winning project scope, and this is the direction the team will continue to pursue.

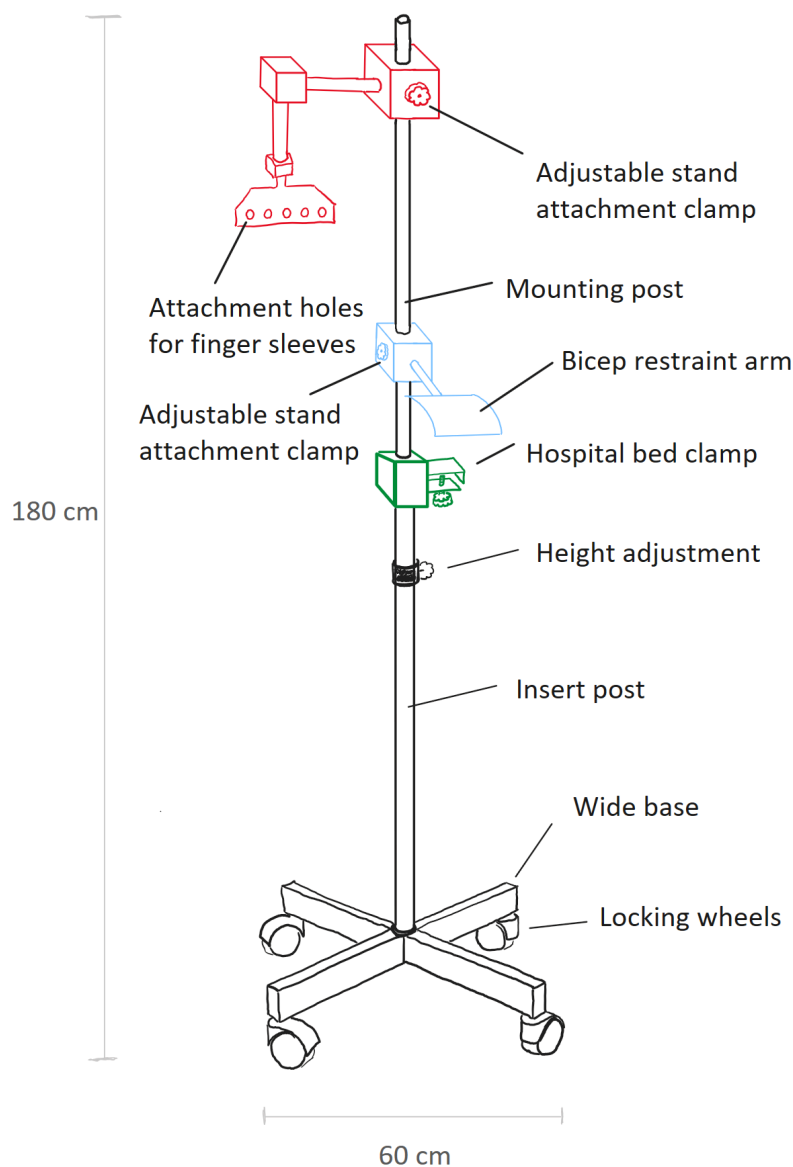


Figure 10: Hybridized final design of mechanical structure

5 FABRICATION

5.1 Materials

Mechanical

For the mechanical component of the design an IV pole was used as the main structural frame, taking advantage of the built-in height adjustment and stability. A sheet of aluminum was selected for the attachment platform since it provides an ideal balance of strength and low weight, allowing the attachment platform to remain stable without making the IV-pole structure top-heavy. The material is easy to machine, which made waterjet cutting and shaping straightforward and efficient during fabrication.

To stabilize the connection between the aluminum piece and the IV pole, custom 3D-printed stoppers fabricated from TPU for flexibility were added to prevent sliding and rotation during use. Bead chains and D-rings were incorporated as the linkage mechanism. Additionally, all materials will be expected to withstand standard cleaning procedures. Daily operating room use and sterilization could begin to erode, rust, or break down materials, so choosing strong and durable materials is important for 3D printing and metal fabrication in order to maintain patient safety over the shelf life of the device.

Finger Sleeve

The finger sleeve portion utilizes a substantial amount of ballistic nylon, an affordable, abundant, and strong plastic material for a majority of its components. Ballistic nylon was ultimately chosen for its overall strength and workability in the overall fabrication process of the finger sleeves. It is crucial that for the overall design stability is ensured throughout the desired shelflife. The nylon portions of the design will need to withstand daily use and intense sanitation. Next, the team chose to implement velcro for the strap component of the design. Velcro is extremely easy to use and will reduce the application time of the finger sleeves prior to a procedure. Finally, the D-Ring is a simple durable plastic ring that will be implemented in the connective elements of the design. This was 3D-printed out of Formlabs general resin v5 due to its high tensile strength and temperature resistance.

5.2 Methods

Mechanical

The entire body and base of the stand was sourced from a Medline Stand IV Pole ordered on Amazon. The stand was assembled by unfolding the base legs and spreading them out until the base was stable, and then assembling the central pole sections by inserting them into one another in the correct order. Once the central sections were connected, the pole's height was adjusted to the desired length and the top-piece was secured and fastened to the apex of the

assembled pole. See Appendix 10.2 (Mechanical Stand Fabrication Protocol) for a more in-depth guide on assembling the stand.

The mounting plate that connects the sleeves to the central mechanical body was created by cutting a sheet of aluminum 3003 alloy using a waterjet in the MakerSpace. A 2D-sketch of the mounting plate design was created in OnShape. See Appendix 10.6 (Mechanical Stand Fabrication Protocol) to view the drawing file. This CAD file was exported to the waterjet machine. The aluminum sheet was then loaded into the waterjet cutter, and the waterjet sliced the mounting plate per the desired pattern. The resulting piece had sharp edges which were dulled using a file in the MakerSpace. See Appendix 10.2 (Mechanical Stand Fabrication Protocol) for a more in-depth guide on the creation of the mounting plate.

The mounting plate stopper was modeled as a 2D-sketch in OnShape. To determine its dimensions, the diameter of the metal hook on the apex of the IV pole was measured. The diameter of the central hole on the stopper was designed to be approximately the same size as the rod it would be fitted onto. The hole was also designed to be hexagonal to limit rotation of the stopper around the rod, allowing for a more secure hold of the mounting plate. Once the stopper was modeled, the 3D CAD file was sent to the MakerSpace and was printed in TPU filament. For further details on the design process for the mounting plate stopper, see Appendix 10.2 (Mechanical Stand Fabrication Protocol).

Finger Sleeve

Using a laser cutter within the MakerLab, a cut out containing five 44 x 1.5 cm rectangles will be cut out of a nylon fabric sheet. The 44 x 1.5 cm nylon strip will be folded into a loop, overlapping the two ends 8 cm onto itself. Using the sewing machine in the MakerLab, careful stitches were made at the terminal ends, still 8 cm onto itself. After that, more stitching was done to create 5-1.6 cm slots between the layers of nylon fabric on each end of the strip, creating ten total. If later testing shows that the stitching material and/or type does not withstand forces to the finger sleeve stated in Appendix 10.1 (Product Design Specification), fabric adhesive can be added to the connections for reinforcement, as well as stronger stitching material. The long end of the strip will be pushed through a 1.5 cm D-Ring seen in Figure 12. Finally, 12.7 x 100 mm double sided velcro strips can be wrapped around the two loops of the finger sleeve, first through the bottom to secure the base of the finger. From there, another double sided velcro strip can be placed through any of the remaining 4 slots, depending on the length and size of the patient's finger. A more detailed protocol is described in Appendix 10.5 (Finger Sleeve Fabrication Protocol).

5.3 Final Prototype

Mechanical

The final mechanical stand prototype displayed in Figure 11 differs from the proposed design in multiple ways. Firstly, the stand has no bicep restraint arm or adjustable bed clamp as these were deemed later in the semester to be lower-yield additions compared to other goals that had been set out to achieve. The stand also transitioned from the wheeled base that was initially proposed to a light-weight, stabilizing base due to a change in the preference of the client. Lastly, the top of the stand became a hook attachment mechanism with a mounting plate suspended from it due to the client selecting a different model for the central body.

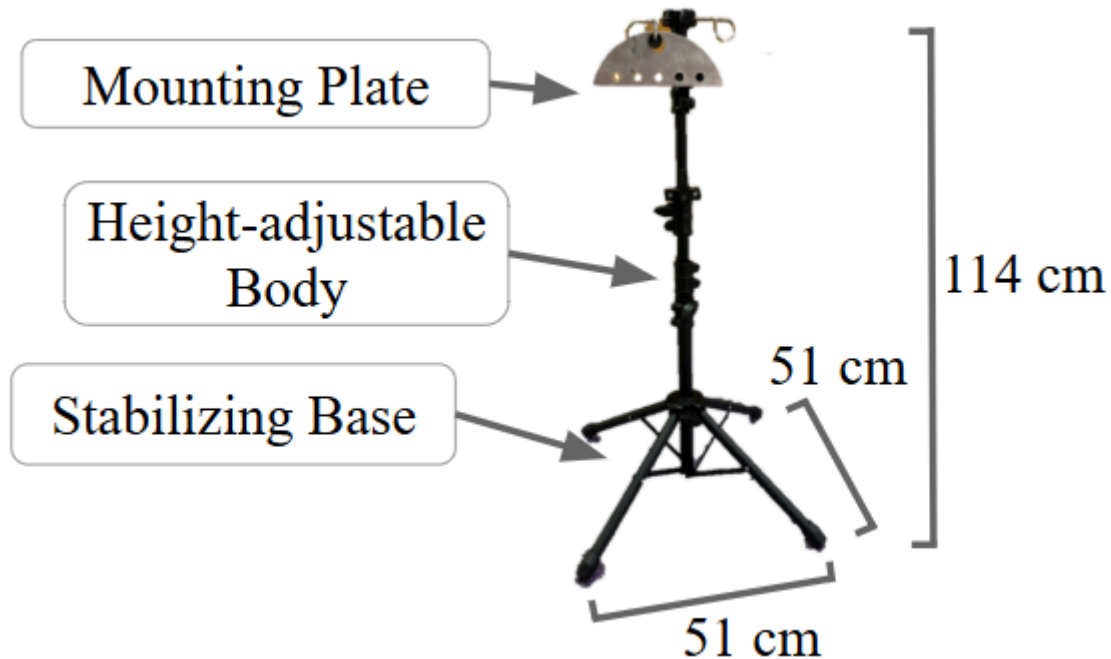


Figure 11: Mechanical Design Final Prototype, displaying stand and mounting plate portions of the design

Finger Sleeve

The final finger sleeve prototype, seen in Figure 12, differs from the proposed design in multiple ways. For one, there is no longer a T shaped outline for the nylon strip. Instead, there is now one long strip that is folded onto itself, described more thoroughly in the methods section and Appendix 10.5 (Finger Sleeve Fabrication Protocol). With that, the adjustable velcro strap no longer slides up and down the strip, but instead can be pulled out of the slot and replaced. Additionally, the velcro straps do not require a separate ring for cinching, but rather feed through a slit in the other end of the velcro strap itself.

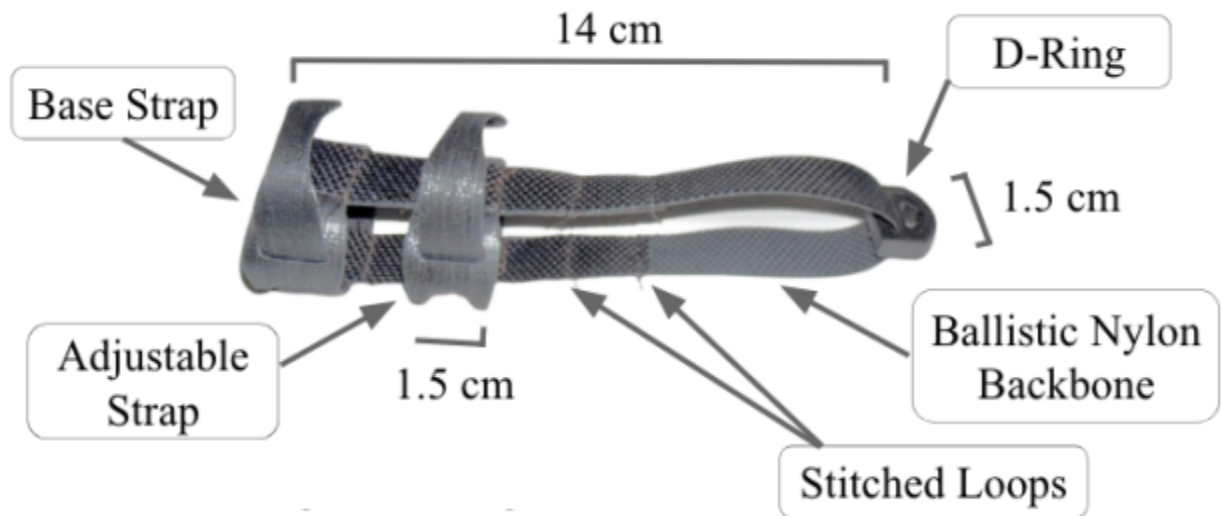


Figure 12: Final finger sleeve prototype

6 TESTING & RESULTS

FEA Analysis

The completed sleeve attachment part was evaluated using finite element analysis (FEA) to confirm that it meets the required safety factor. All applied forces were multiplied by four to represent a factor of safety of 4 during loading. Under these conditions, the model reached a maximum von Mises stress of $5.2 \times 10^6 \text{ N/m}^2$, which is well below the material's yield strength of $4.1 \times 10^7 \text{ N/m}^2$. The FEA heat map, seen in Figure 13, showed that the highest stresses occurred in localized areas and did not approach the yield limit. Overall, the results indicate that the part remains safely within the elastic range even under the amplified loading and meets the intended safety requirements.

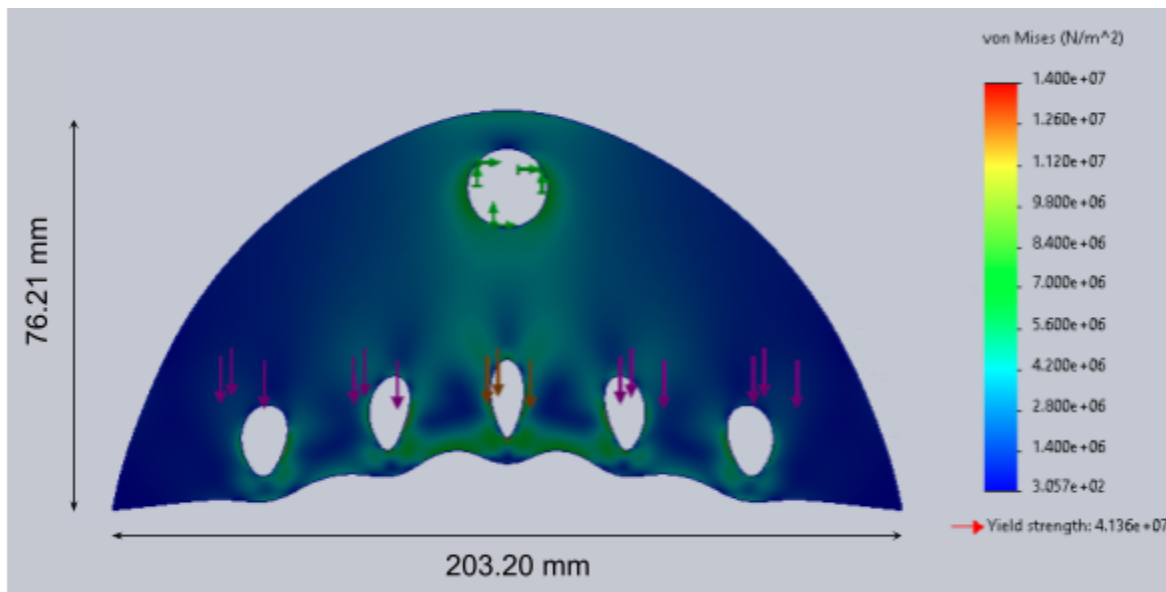


Figure 13: FEA results showing the stress distribution of the part under $4\times$ loading. The model is 0.88 mm thick and reached a maximum von Mises stress of $5.2 \times 10^6 \text{ N/m}^2$, below the material yield strength of $4.1 \times 10^7 \text{ N/m}^2$.

Autoclaved Tensile Testing

To determine the tensile strength of ballistic nylon and the effects of autoclaving the material 3 identical dog bone shaped strips of ballistic nylon were tested under each of the three conditions: no autoclave (control), 1 autoclave cycle, and 5 autoclave cycles. Since the final finger sleeve design consists of two $15 \times 0.4 \text{ mm}$ strips and must hold 44 N of tensile force, stated in Appendix 10.1 (Product Design Specification), ballistic nylon must have a maximum tensile stress of 20 MPa. Due to the thickness of the fabric, it was laser cut into dog bone shaped strips, provided in Appendix 10.11 (Dog Bone CAD Drawing), dimensioned to align with ASTM D882 standards [11] for tensile testing thin plastics ($<1 \text{ mm}$). This allowed for consistent and

accurate calculations of stress and strain across all samples. Tensile testing was then conducted on all 9 strips and the MTS machine recorded load (N), displacement (mm), and time (s) of each test. This raw data, detailed in Appendix 10.9 (Autoclaved Tensile Testing Raw MTS Data), was converted into stress strain curves, which are overlaid on a graph in Figure 14. A more detailed protocol for this testing can be found in Appendix 10.8 (Autoclaved Tensile Testing Protocol).

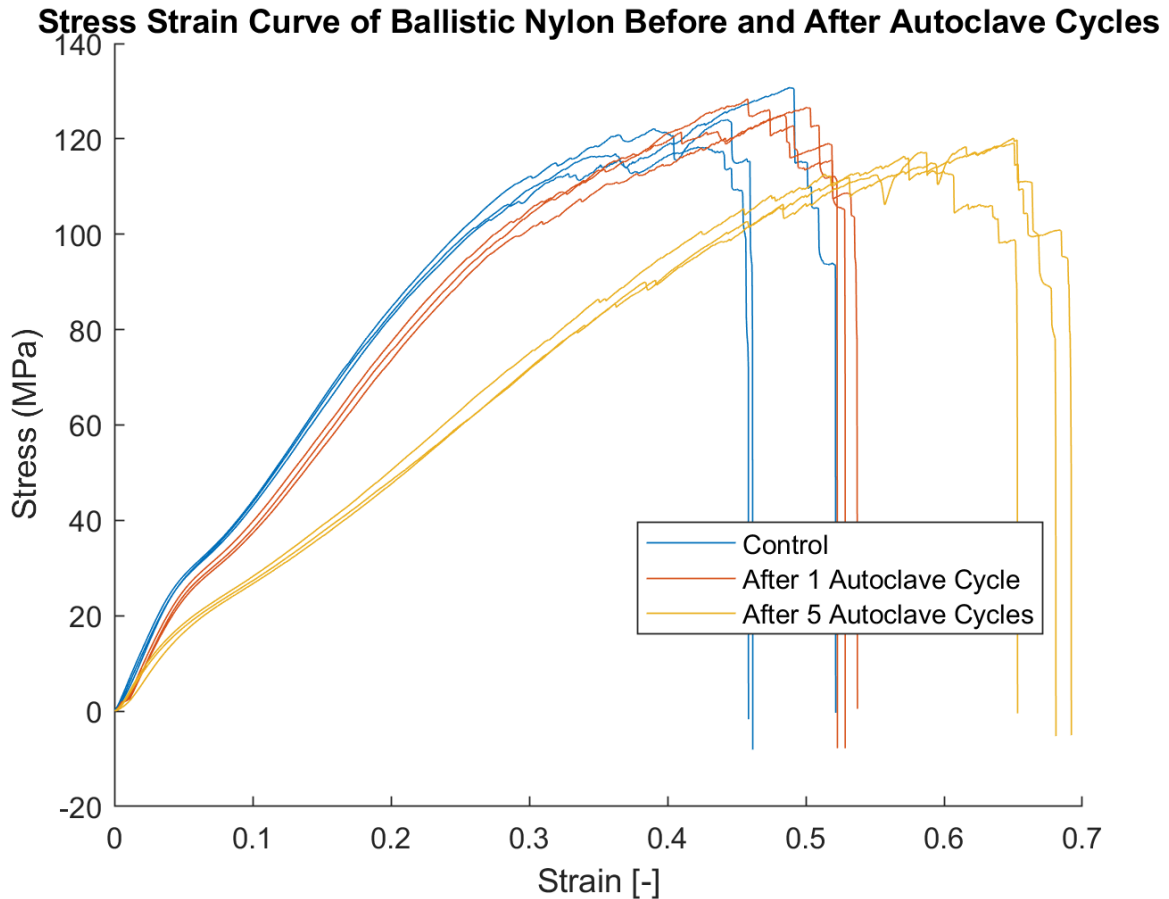


Figure 14: Stress (MPa) vs. strain curve of ballistic nylon before and after varying cycles in a 250 °F gravity autoclave. The blue lines represent the control material which was never autoclaved and MTS tested directly after being laser cut. The red lines represent the material that was put through one autoclave cycle and the yellow lines represent the material that was put through 5 autoclave cycles.

Independent two-tailed T-tests were used to analyze the change in elastic modulus between the control and 1 cycle ($p = 0.0038$), control and 5 cycles ($p = 2.2950e-6$), and 1 cycle and 5 cycles ($p = 2.9005e-4$). Since the elastic modulus significantly decreased, visualized in Figure 15, it was determined that autoclaving ballistic nylon causes it to become less stiff and deform under smaller loads. Similarly, independent two-tailed T-tests were used to analyze the change in failure strain between the control and 1 cycle ($p = 0.0796$), control and 5 cycles ($p =$

0.0012), and 1 cycle and 5 cycles ($p = 8.2444\text{e-}6$). Since the failure strain significantly increased, visualized in Figure 16, it was determined that autoclaving ballistic nylon causes it to become more ductile. Finally, autoclaving was expected to only decrease the maximum stress, independent single-tailed T-tests were used to analyze the change in maximum stress between the control and 1 cycle ($p = 0.2844$), control and 5 cycles ($p = 0.1049$), and 1 cycle and 5 cycles ($p = 0.0018$). Due to the significant change in maximum stress between 1 cycle and 5 cycles, visualized in Figure 17, it was determined that the ultimate strength of ballistic nylon decreases when autoclaved. All of these statistical analyses were performed using MATLAB code, further detailed in Appendix 10.10 (Autoclaved Tensile Testing MATLAB Code).

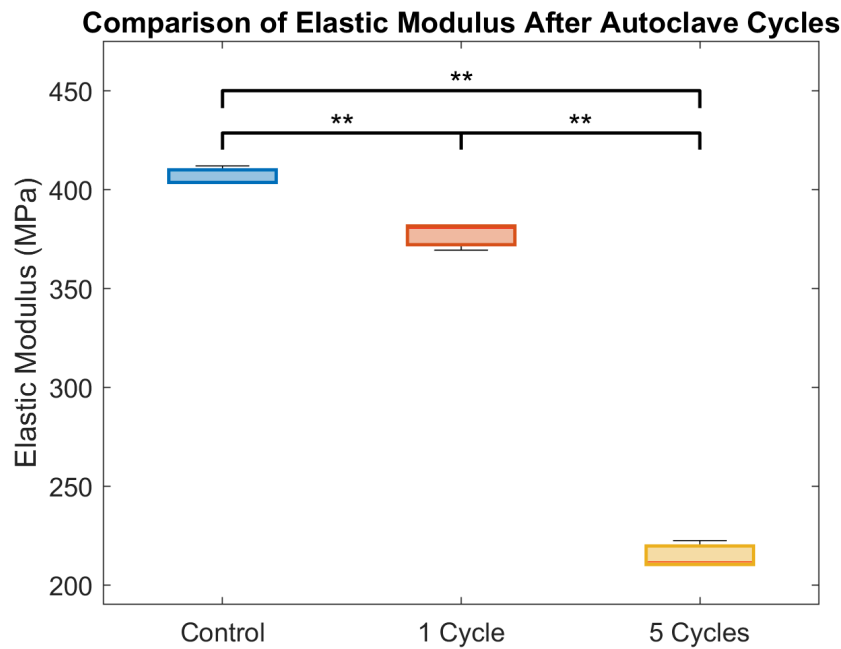


Figure 15: Box plot comparing the elastic modulus (MPa) of each group (Control, 1 Cycle, and 5 Cycles). Each group contains 3 samples. The groups were compared to one another using independent two-tailed T-tests. Brackets: * = p -value < 0.05 , ** = p -value < 0.01

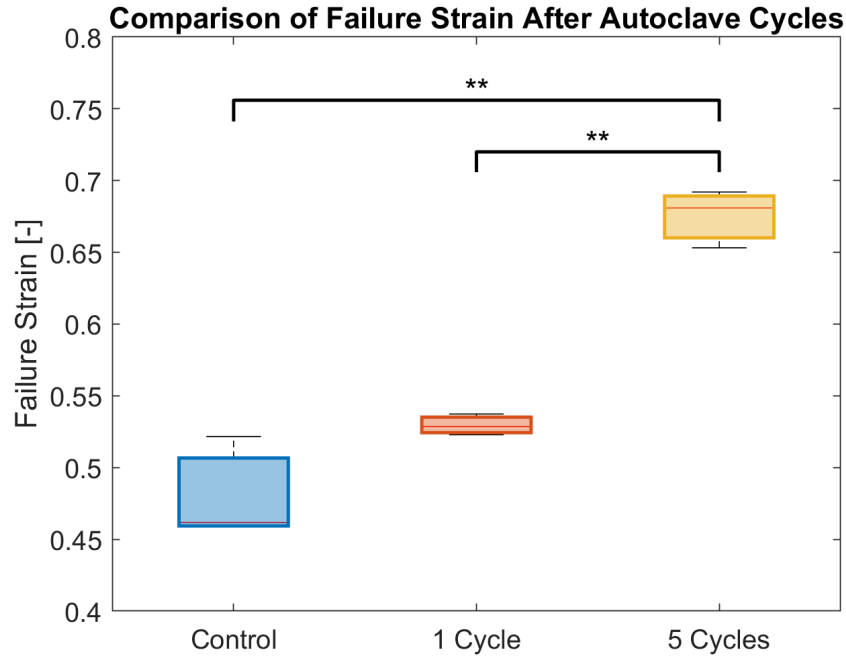


Figure 16: Box plot comparing the strain at the point of failure for each group (Control, 1 Cycle, and 5 Cycles). Each group contains 3 samples. The groups were compared to one another using independent two-tailed T-tests. Brackets: * = p-value <0.05, ** = p-value <0.01

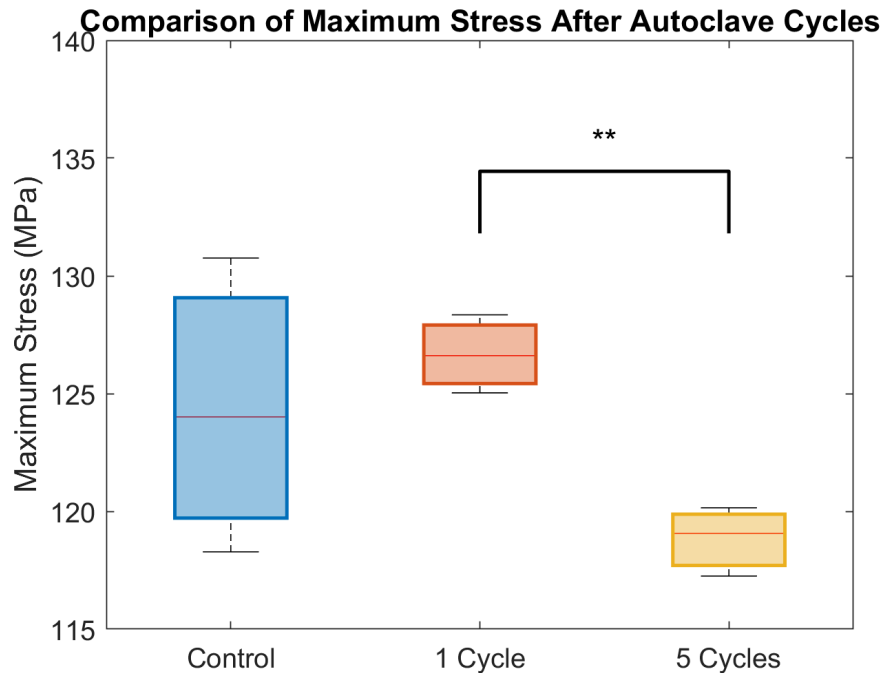


Figure 17: Box plot comparing the maximum stress (MPa) for each group (Control, 1 Cycle, and 5 Cycles). Each group contains 3 samples. The groups were compared to one another using independent single-tailed T-tests. Brackets: * = p-value <0.05, ** = p-value <0.01

Slippage Testing

The finalized finger sleeve was then tested with the goal of determining the safety and overall effectiveness of the prototype. The sleeve was hung by a hook to simulate the metal beads used in the final design. Next, to fully stress one sleeve to its maximum load only one sleeve was tested at a time. Each finger was placed in the device for 10 total minutes and overall slip displacement was measured in millimeters. Test protocol is further detailed in Appendix 10.12 (Slippage Testing Protocol). Two participants had noticeably different hand lengths and girths, highlighted in Appendix 10.13 (Slippage Testing Raw Data). On average, the total finger sleeves slippage displacement across 8 trials was 1.04mm for the 10 minute load cycle. The maximum recorded slip was 2.2 mm and in a few instances no slip occurred at all. Additionally, it was noted in observation that during the testing, the majority of the slippage occurred as the finger sleeve experienced the initial load, highlighting the importance of correctly applying the sleeve.

Stitched Tensile Testing

To determine the tensile strength of the stitching material and pattern used for the finger sleeve, identical dog bone shaped strips of ballistic nylon used for the autoclaved tensile testing, provided in Appendix 10.11 (Dog Bone CAD Drawing), were used but cut them in half. The same stitch used on the finger sleeve prototype was used then to stitch the two halves together. Tensile testing with the MTS machine proved that the stitching could handle tensile stress greater than 20 MPa. To determine the effects of autoclaving on the stitches, three stitched dog bones were autoclaved and three were not. Tensile testing was then conducted on all 6 strips and the MTS machine recorded load (N), displacement (mm), and time (s) of each test. This raw data, detailed in Appendix 10.15 (Stitched Tensile Testing Raw MTS Data), was converted into stress strain curves, which are overlaid on a graph in Figure 18. A more detailed protocol for this testing can be found in Appendix 10.14 (Stitched Tensile Testing Protocol). Independent two-tailed T-tests showed no significant change in elastic modulus ($p = 0.0698$) or failure strain ($p = 0.0948$) between the two groups. Additionally, since it was only expected for the maximum stress to decrease, an independent single-tailed T-test was used to determine that there was no significant decrease in maximum stress ($p = 0.2923$) between the two groups. All of these statistical analyses were performed using MATLAB code detailed in Appendix 10.16 (Stitched Tensile Testing MATLAB Code).

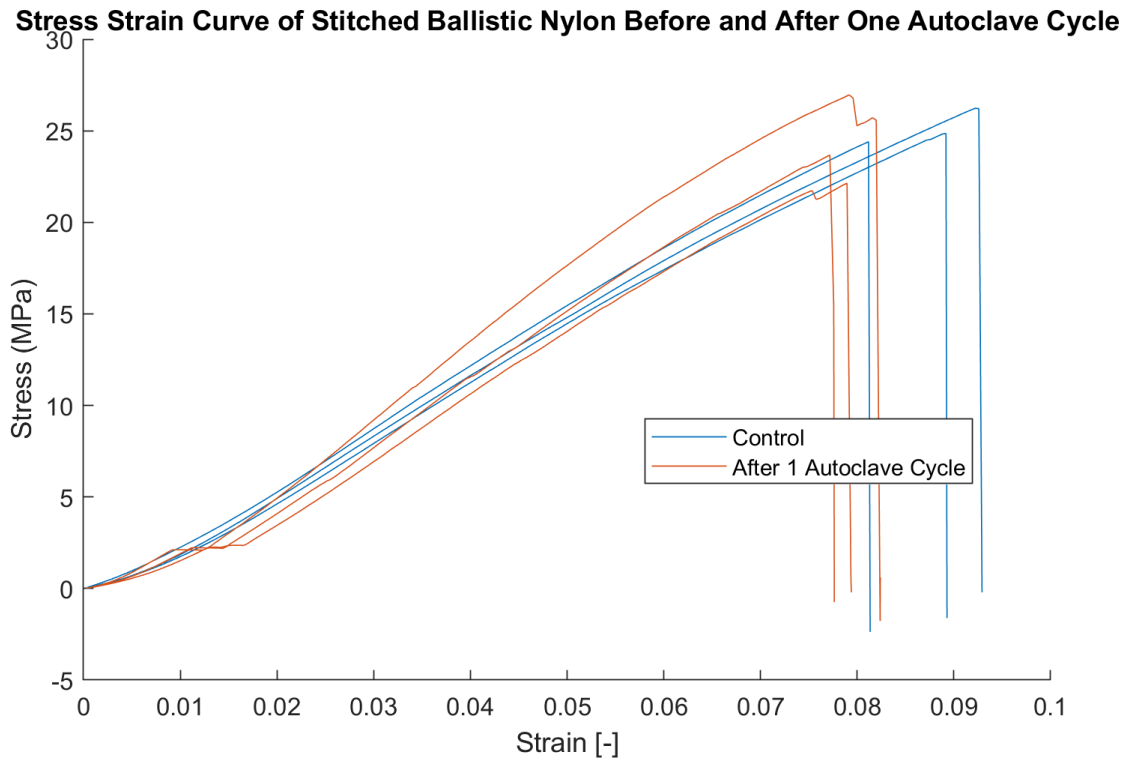


Figure 18: Stress (MPa) vs. strain curve of stitched ballistic nylon before and after varying cycles in a 250 °F gravity autoclave. The blue lines represent the control material which was never autoclaved and MTS tested directly after being laser cut and stitched. The red lines represent the material that was put through one autoclave cycle.

7 DISCUSSION

The results of the mechanical, tensile, and slippage testing demonstrate that the proposed traction device is both feasible and capable for clinical use in Senegal.

MTS testing of autoclaved ballistic showed a significant decrease in elastic modulus, as well as an increase in failure strain. This can be explained by the absorption of steam during the autoclave process. Nylon is a hygroscopic molecule, which absorbs water through hydrogen bonding [12]. During the autoclave process, the nylon is exposed to pressurized water, placing it in a plasticized state. The material becomes more flexible and ductile, while also retaining the majority of its strength, because only Hydrogen bonds are created and no bonds of the nylon material are broken [12]. Overall, these findings demonstrate that the observed changes are driven by reversible moisture induced plasticization, rather than permanent material degradation. Even so, the long term effects of repeated moisture absorption on material durability warrant further investigation. The team can only confidently support 5 uses of a finger sleeve before replacement without further testing. However, it is expected that the finger sleeves can withstand

many more uses as the average maximum stress after 5 autoclaves (118.9 MPa) is almost 6 times greater than the required maximum stress of the finger sleeve (20 MPa).

The minimal average displacement measured during the slippage testing indicates that the sleeves effectively performed as intended. The device successfully supported an average human arm load of approximately 60 N with little to no resulting moment. As outlined in Appendix 10.1 (Product Design Specification), the target load capacity for each sleeve was 22–44 N without slipping, tearing, or deforming. Based on the test results, the sleeves fully met and exceeded this requirement, supporting the desired forces without any signs of degradation.

The tensile testing of the stitched ballistic nylon was determined to not accurately represent the forces that would be applied to the stitching during axial loading of the finger sleeves. Due to the configuration of the stitching in the finger sleeve, it is expected that the ballistic nylon backbone would absorb the majority of the force, leaving unpredictable indirect forces on the stitching. This force would be distributed throughout 10 separate stitches along the length of the finger sleeve. Since a singular stitch under direct load had an average maximum stress of 25.2 MPa, it is assumed that the stitching in the finger sleeve will also be able to safely handle the target load capacity, but further testing should be conducted to confirm this idea. From this testing, it can be concluded that autoclaving has no effect on the strength of the stitching itself, as no significant deviations ($p < 0.05$) occurred in maximum stress, elastic modulus, or failure strain.

The mechanical structure safely supported the required loads with an adequate factor of safety, implying the device can reliably replace manual traction methods, reducing clinician fatigue and improving the precision of procedures. Ethical considerations were central to both the development and intended clinical applications of this device. Since hospitals in Senegal often face equipment shortages and socioeconomic inequality in healthcare access [13], the design prioritizes affordability, reproducibility, and equitable distribution. The device uses low-cost, biocompatible, and cleanable materials allowing for reuse with low infection risks in high-patient volume settings [14]. Evaluation testing prompted several iterative changes and highlighted areas requiring further refinement. The originally proposed bicep restraint and integrated bed clamp were removed due to limited benefit compared with the increased fabrication complexity. Future improvements should include testing additional stabilizing components, such as a more robust base or clamp attachment. A source of error in the FEA analysis was that it failed to account for load duration and load cycling providing space for future development in testing methodology.

8 CONCLUSION

Orthopedic injuries to the upper extremity are highly prevalent and often require expert medical treatment due to their anatomical complexity. A key instrument utilized in the treatment of these injuries is a digital traction device, which is used in a plethora of surgical and rehabilitative settings to both stabilize the upper extremity and relax the regions of the body requiring treatment. This report proposes a digital traction device with several distinct advantages. These include its affordability compared to other market options, its manufacturability due to its simple design, and its versatility in a plethora of hospital settings.

While the final design creates a solid foundation for a digital traction system that could be used by the client, the existing prototype still requires future work. For the mechanical body, testing the reinforcing materials such as the beads and silicone grippers would help ensure all aspects of the design meets the team's factor of safety requirements and can withstand the forces that shall be exerted upon them in a hospital setting. There are also stabilization options that could be added to the mechanical body to further reduce risk of the device tipping, including a bed clamp which would fasten the mechanical body to the hospital beds and the operating table.

The final design of the finger sleeve also requires continued testing and refinement. The reusability of the sleeve was only tested up to five autoclave cycles, and the team's goal was to have the sleeves be adequate through 50 cycles. While the sleeves maintained their strength through five cycles, testing them beyond just five would either demonstrate the longevity of the current design or provide evidence that the current sleeve requires additional reinforcement. Also, additional testing of stitching parameters including the type, thread, density, and pattern will be necessary in order to optimize the strength of the sleeve.

Overall, the achievements of the final design lay the groundwork for the creation of a more affordable and versatile digital traction system. With further development of the model, it promises an exciting future for low-resource hospitals seeking to better treat orthopedic injuries of the upper extremity.

9 REFERENCES

- [1] V. Candela, P. Di Lucia, C. Carnevali, A. Milanese, A. Spagnoli, C. Villani, and Stefano Gumina, “Epidemiology of distal radius fractures: a detailed survey on a large sample of patients in a suburban area,” *Journal of Orthopaedics and Traumatology*, vol. 23, no. 1, p. 43, Aug. 30, 2022. DOI: 10.1186/s10195-022-00663-6. [Online]. Available: <https://pmc.ncbi.nlm.nih.gov/articles/PMC9428104/>
- [2] B. Choudhry, B. Leung, E. Filips, and K. Dhaliwal, “Keeping the Traction on in Orthopaedics,” *Cureus*, vol. 12, no. 8, Article e10034, Aug. 2020. DOI: 10.7759/cureus.10034. [Online]. Available: <https://pmc.ncbi.nlm.nih.gov/articles/PMC7515792/>
- [3] D. Haughton, D. Jordan, M. Malahias, S. Hindocha, and W. Khan, “Principles of hand fracture management,” *Open Orthop J*, vol. 6, pp. 43–53, 2012, doi: 10.2174/1874325001206010043.
- [4] M. Soumah, 'Digital Traction - Condensed Questions from Previous Email and Meeting', 2025
- [5] “Hand Fixation» Reison Medical®,” Reison Medical, Apr. 08, 2025. <https://reison.se/product/hand-fixation/> (accessed Sep. 30, 2025).
- [6] K. Akhtar, D. Akhtar, and J. Simmons, “A readily available alternative to Chinese finger traps for fracture reduction,” *Royal College of Surgeons of England*, <https://publishing.rcseng.ac.uk/doi/full/10.1308/rcsann.2013.95.2.159> (accessed Sep. 9, 2025).
- [7] A. Zolotov, “Handmade Traction Wrist Tower,” *J Wrist Surg*, vol. 7, no. 5, pp. 441–444, Nov. 2018, doi: 10.1055/s-0038-1649504.
- [8] “Fig. 3. The bone structure of the human hand including the forearm and...,” ResearchGate. Accessed: Oct. 06, 2025. [Online]. Available: https://www.researchgate.net/figure/The-bone-structure-of-the-human-hand-including-the-forearm-and-wrist-1-7-CMC_fig1_369946938
- [9] M. Zhang and A. F. Mak, “In vivo frictional properties of human skin and five materials: aluminium, nylon, silicone, cotton sock, Pelite,” *Prosthetics and Orthotics International*, vol. 23, no. 2, pp. 135–141, Aug. 1999. DOI: 10.3109/03093649909071625. [Online]. Available: <https://pubmed.ncbi.nlm.nih.gov/10493141/>
- [10] “Pape Samb – Jamarek.” Accessed: Oct. 05, 2025. [Online]. Available: <https://jamarek.org/wps-members/petter-nilsen/>

[11] MTS Systems Corporation, “ASTM D882 Tensile Properties of Thin Film / Plastic Sheeting: Test Method Summary,” Technical Note 100-332-870a, Eden Prairie, MN, USA, Aug. 2023.

[12] D. Mesyn, “Managing Moisture: The Science Behind Moisture Absorption in Nylon.” Accessed: Nov. 18, 2025. [Online]. Available: <https://etp.teknorapex.com/blog/moisture-absorption-in-nylon>

[13] R. M. Oosting, L. S. G. L. Wauben, R. S. Groen, and J. Dankelman, “Equipment for essential surgical care in 9 countries across Africa: availability, barriers and need for novel design,” *Health Technology*, vol. 5, no. 2, pp. 112–116, 2018. [Online]. Available: <https://link.springer.com/article/10.1007/s12553-018-0275-x>

[14] Y. Chan, L. Banza, C. Martin Jr., and W. J. Harrison, “Essential fracture and orthopaedic equipment lists in low resource settings: consensus derived by survey of experts in Africa,” *BMJ Open*, vol. 8, no. 9, p. e023473, 2018. [Online]. Available: <https://pmc.ncbi.nlm.nih.gov/articles/PMC6144338/>

10 APPENDIX

10.1 Product Design Specification

Function

Design a device that allows for precise digital control and support of the components of the human hand through the use of Japanese finger sleeves or a similar universal type of support. This device will be designed to allow for controlled and stable traction during relevant procedures so that proper positioning of the hand can be attained with minimal manual effort.

Client requirements

- The device must support the patient's hand for approximately 50 minutes during fracture casting and be usable during surgery.
- Patients lie with their elbows bent at 90° and their hands suspended by finger sleeves; the sleeves must not compress the fingers, as this could cause stiffness.
- Reusable (due to economic constraints, single-use is not feasible), sterilizable design required.
- Materials must be:
 - Strong, elastic, and latex-free (non-allergenic).
 - MRI-compatible (no metal components).
- Sizing:
 - Multiple sleeve sizes needed.
 - An adaptive "one-size-fits-all" or an adjustable option are preferred.
- Functionality:
 - Provide a high-friction grip to allow stabilization and dexterity during traction and surgical use without restricting circulation.
 - The design must allow for the natural flexion and extension of finger joints, ensuring the tendons can glide smoothly within their sheaths during any minor patient movement or adjustment [1].
- Smart/Innovative features (desired but not mandatory):
 - Sensors to track finger pressure, bending angles (0–90°), and usage duration.
 - Alert system if complications occur: optional.
- Must be durable, cost-effective, and suited for high patient volume (~25,000 orthopedic patients every 6 months).
- No copyright required; aim for a "modern, smarter" tool.

Design requirements

1. Physical and Operational Characteristics

a. Performance requirements

- i. The sleeve must securely support the full weight of a patient's hand and forearm through a single fingertip without tearing, stretching permanently, or slipping off. The team's target is for the sleeves to support a static load of at least 22-44 N per finger as a safety factor.
- ii. The device must maintain its elasticity, strength, and surface texture through a minimum of 50 cycles of use and sterilization.
- iii. The inner surface of the sleeves must provide sufficient friction to prevent the finger from slipping more than 5 mm under load.
- iv. The outer attachment point must securely hold the suspension mechanism.
- v. The sleeve material must stretch to accommodate various finger diameters, with the team's goal being a 15-25% stretch beyond a relaxed state. This retraction should be enough to provide a secure and snug fit while not being so tight that it causes harmful or uncomfortable finger constriction.
- vi. If implemented, the device will have "smart" monitoring capability that measures the traction force in each finger. The target shall be to keep the displayed force within 0.5–5 N of the actual load in order to accurately detect delicate manipulation or alert the physician if a dangerous level of force is being applied. The sensor would also have integrated wireless (e.g., Bluetooth) transmission for real-time data analysis.

b. Safety

- i. All materials must be medical-grade, non-toxic, and hypoallergenic (specifically latex-free) to avoid skin irritation or allergic reactions.
- ii. The design must avoid finger compression to prevent cutting off circulation (ischemia) or causing nerve damage during the 50-minute procedure.
- iii. The entire device must be made from non-metallic, MRI-compatible materials to ensure it is not a projectile risk and does not generate heat or artifacts that could harm the patient or corrupt imaging data.
- iv. The device must be designed and tested to have a significantly higher load-bearing capacity than expected in use to prevent catastrophic failure (e.g., tearing) that could result in patient injury from a falling arm.
- v. The design and materials must be compatible with standard hospital sterilization techniques (e.g., steam autoclave, chemical sterilants) without degrading, to prevent cross-contamination between patients.

c. Accuracy and Reliability

- i. If multiple sizes are produced, each size must consistently and accurately fit the intended range of finger diameters.
- ii. If one size is used the device should consistently avoid slippage for all finger sizes and be controlled to under 5 total millimeters of displacement for an entire procedure.
- iii. Any integrated sensors that are implemented (e.g., for force) must provide accurate and repeatable readings within the specified target ranges (e.g., ± 0.1 N accuracy for force sensing) to be clinically useful for monitoring.

d. Life in Service

- i. The finger sleeves must reliably perform at least 50 full uses and autoclave sterilization cycles over their service lifetime.
 - 1. Idrissa Pouye General Hospital receives 25,000 orthopedic patients every 6 months. Assuming that 17.5% of all orthopedic visits are DRFs, the finger sleeves will be used about 8750 times per year [2].
 - 2. The finger sleeves should maintain full function for 0.25 years.
 - 3. There will be a stock of 40 sets of finger sleeves assuming 25 DRFs per day and a 1.5x sterilization turnover buffer.
- ii. Elastic and sensor components should endure 100,000 loading cycles within the expected operating force range (22-44 N), with sensor accuracy drift less than $\pm 5\%$ [3].

e. Shelf Life

- i. In storage, device components should retain functionality for at least 3 years under temperatures between 10-30 °C, in relative humidity less than 70%, and away from direct UV light.

f. Operating Environment

- i. Device must function in standard operating room conditions: 20-24 °C, 20-60% relative humidity [4].
- ii. Surfaces should be resistant to corrosion or degradation by blood, saline, antiseptics, and common disinfectants.
- iii. Device must be able to tolerate occasional jostling or movement without loss of alignment or sensor calibration.
- iv. Device must be MRI compatible with no ferromagnetic metal parts and any electronics shielded or safely located to avoid interfering with imaging.

g. Ergonomics

- i. Limit peak interface pressure to 50 N/cm², below reported pressure pain thresholds [5].

- ii. Inner finger sleeves must provide a coefficient of friction of 0.4 under standard operating room conditions to ensure grip, while remaining below 1.0 to avoid excessive shear and possible skin damage [6].
- iii. Limit axial traction force per digit to 50 N to avoid excessive loading on finger joints and the DRF site [7].

h. Size

- i. The device must fit within the surgical field without interfering with other instruments [8].
- ii. Should accommodate all hand and finger sizes specifically for the Senegalese whose typical finger size is 8.26 cm for females and 8.69cm for males [9].
- iii. Must be compact enough to not block MRI coils or distort imaging [10].
- iv. Adjustability is an important component, both to increase or decrease tension or create smaller or larger overall structure [11].

i. Weight

- i. Must be lightweight for easy handling and help reduce surgical fatigue in a delicate surgical procedure.
- ii. Heavier components risk displacement forces within the MRI machine. Therefore, lower weight improves safety [12].
- iii. Smaller and lighter Japanese finger sleeve components means less surface area contact with skin, reducing risk of irritation [13].

j. Materials

- i. Materials must be non-ferromagnetic, non-conductive, and biocompatible. Plastics, ceramics or composites, as well as titanium are all possible materials. They must be able to handle sterilization methods [14].
- ii. No material can be irritable to the skin, causing redness, swelling, burning, or itching [15].

k. Aesthetics, Appearance, and Finish

- i. Must be finished with a non reflective material, which will avoid glare from surgical lights.
- ii. Include any padding where soft tissue would ever come into contact with solid material, for patient safety.
- iii. The device has no major need to be aesthetically pleasing, as it will need to be more functional than anything.

2. Production Characteristics

a. Quantity

- i. The client's goal for the project is to develop a single digital traction device that aids performance and reduces the difficulty of standard orthopedic hand and wrist procedures. The product should be able to accurately manipulate finger tension in both the right and left hands during

surgery while still allowing the client to easily maintain its function and sanitation through extensive use.

b. Target Product Cost

- i. The client has not given the project a set budget yet for prototyping. They indicated that would be covered as materials and resources are required throughout the project.
- ii. The university allots a budget of \$50 for use in the Design Labs.
- iii. The device is intended for use in a hospital in Senegal, where economic resources are more limited, roughly 40 times lower GDP per capita than the US. The end product should be relatively lower in cost compared to similar products on the market [16].

3. Miscellaneous

a. Standards and Specifications

i. International Standards

1. ISO 13485:2016: Medical devices: Quality management systems [17]
 - a. Covers requirements for the quality management system for medical devices. Globally recognized and expected by regulators worldwide.
2. ISO 14971:2019: Medical devices: Application of risk management to medical devices [18]
 - a. Methodology for identifying, evaluating, and controlling device risks.
3. ISO 10993-1:2018: Biological evaluation of medical devices: Evaluation and testing within a risk management process [19]
 - a. Provides framework for biological safety assessment of materials in contact with the patient's skin or body.
4. ISO 15223-1:2021: Medical devices: Symbols to be used with information to be supplied by the manufacturer [20]
 - a. Standardized labeling.

ii. United States Additional Regulations

1. 21 CFR Part 820: Quality System Regulation [21]
 - a. The FDA's legally binding quality management regulation for medical devices marketed in the U.S.

b. Customer

- i. The potential customers for this device include teaching hospitals, surgical centers, rehabilitation clinics, and any other medical facility that performs upper-extremity orthopedics. At this stage, the client will be the primary source used to validate the device's ability to securely hold individual fingers and apply precise, adjustable traction to each digit. Since the

device is intended for use in resource-constrained settings such as Idrissa Pouye General Hospital in Senegal, the customer is particularly interested in a cost-conscious and sterilizable design that minimizes the need for replacement. They are also looking for a modular approach that allows a single device to be compatible with MRI and accommodate a wide range of finger sizes. Long-term, the customer envisions expanding use of the device to other medical facilities where reproducible digital traction would improve workflow and clinical outcomes.

c. Patient-related concerns

- i. This device will be used during delicate orthopedic procedures where precise hand positioning is essential, making patient safety a top priority. To protect patients from injury, the design must maintain structural integrity under duress and also provide consistent traction forces without exceeding safe limits for finger joints. This means the sleeves must support the full weight of the patient's upper arm while avoiding any sort of constriction that could cut off circulation or cause nerve injury. The materials used in the device must be medical-grade, hypoallergenic, and non-metallic to prevent skin irritation and ensure MRI compatibility. Also, the device's surfaces must resist degradation from blood, saline, and any disinfectants common to a medical setting.

d. Competition

- i. Competing Design #1: MPR Hand Traction System [22]
 1. The MPR Hand Traction System is a modular device that suspends the patient's hand using finger traps and an adjustable frame that allows stable positioning during orthopedic procedures of the upper extremity surgeries. It also offers adjustable traction and can accommodate a wide range of hand sizes.
 2. While the product fits many of the client's criteria, it provides limited adjustability for fine-tuning individual finger forces and also has a metal frame that makes it incompatible with MRI environments. Furthermore, MPR does not list the cost of the device publicly due to prices being negotiated on a contract basis, making it difficult to assess its affordability for resource-limited hospitals.

iii. Competing Design #2: Standard Finger Trap Suspension Systems [23]

1. This device uses a stainless steel chain-and-pulley mechanism to distribute traction weight across three or more digits and prevent overloading of a single finger.

2. The system is fully autoclavable, making it a common option for hospitals that are looking to avoid single-use devices.
3. Although this option is simple, it again lacks the ability to independently adjust traction forces for each finger and also does not offer any built-in monitoring to ensure consistent loading. This can lead to variability and makes it difficult to replicate the specific traction conditions needed for delicate upper extremity procedures.

References

- [1] "Flexor tendon mechanism," AO Foundation, 2019. [Online]. Available: <https://surgeryreference.aofoundation.org/orthopedic-trauma/adult-trauma/further-reading/hand-flexor-tendon-mechanism>. [Accessed: Dec. 3, 2024].
- [2] V. Candela, P. Di Lucia, C. Carnevali, A. Milanese, A. Spagnoli, C. Villani, and Stefano Gumina, "Epidemiology of distal radius fractures: a detailed survey on a large sample of patients in a suburban area," *Journal of Orthopaedics and Traumatology*, vol. 23, no. 1, p. 43, Aug. 30, 2022. DOI: 10.1186/s10195-022-00663-6. [Online]. Available: <https://pmc.ncbi.nlm.nih.gov/articles/PMC9428104/>
- [3] B. Choudhry, B. Leung, E. Filips, and K. Dhaliwal, "Keeping the Traction on in Orthopaedics," *Cureus*, vol. 12, no. 8, Article e10034, Aug. 2020. DOI: 10.7759/cureus.10034. [Online]. Available: <https://pmc.ncbi.nlm.nih.gov/articles/PMC7515792/>
- [4] ASHRAE, ANSI/ASHRAE/ASHE Standard 170-2017: Ventilation of Health Care Facilities, American Society of Heating, Refrigerating and Air-Conditioning Engineers, Atlanta, GA, USA, 2017.
- [5] Moon Young Park, Doyeon Han, Jung Ho Lim, Min Kyung Shin, Young Rok Han, Dong Hwan Kim, Sungsoo Rhim, and Kyung Sook Kim, "Assessment of pressure pain thresholds in collisions with collaborative robots," *PLoS ONE*, vol. 14, no. 5, Article e0215890, May 02, 2019. DOI: 10.1371/journal.pone.0215890. [Online]. Available: <https://journals.plos.org/plosone/article?id=10.1371/journal.pone.0215890>
- [6] M. Zhang and A. F. Mak, "In vivo frictional properties of human skin and five materials: aluminium, nylon, silicone, cotton sock, Pelite," *Prosthetics and Orthotics International*, vol. 23, no. 2, pp. 135–141, Aug. 1999. DOI: 10.3109/03093649909071625. [Online]. Available: <https://pubmed.ncbi.nlm.nih.gov/10493141/>
- [7] B. Choudhry, B. Leung, E. Filips, and K. Dhaliwal, "Keeping the Traction on in Orthopaedics," *Cureus*, vol. 12, no. 8, Article e10034, Aug. 2020. DOI: 10.7759/cureus.10034. [Online]. Available: <https://pmc.ncbi.nlm.nih.gov/articles/PMC7515792/>
- [8] ASTM International, *Standard Practice for Marking Medical Devices and Other Items for Safety in the Magnetic Resonance Environment*, ASTM F2503-20, West Conshohocken, PA, USA, 2020.
- [9] N. E. Sahin, Rukiye Sumeyye Bakici, S. Toy, and Z. Oner, "Evaluation of Hand Morphometry in Healthy Young Individuals from Different Countries," *International Journal of Morphology*, vol. 42, no. 4, pp. 991–998, Aug. 2024, doi: <https://doi.org/10.4067/s0717-95022024000400991>.
- [10] ASTM International, *Standard Practice for Marking Medical Devices and Other Items for Safety in the Magnetic Resonance Environment*, ASTM F2503-20, West Conshohocken, PA, USA, 2020.
- [11] A. Zolotov, "Handmade Traction Wrist Tower," *J Wrist Surg*, vol. 7, no. 5, pp. 441–444, Nov. 2018, doi: 10.1055/s-0038-1649504.

[12] ASTM International, *Standard Practice for Marking Medical Devices and Other Items for Safety in the Magnetic Resonance Environment*, ASTM F2503-20, West Conshohocken, PA, USA, 2020.

[13] International Organization for Standardization, *Biological Evaluation of Medical Devices—Part 23: Tests for Irritation*, ISO 10993-23:2021, Geneva, Switzerland, 2021.

[14] ASTM International, *Standard Practice for Marking Medical Devices and Other Items for Safety in the Magnetic Resonance Environment*, ASTM F2503-20, West Conshohocken, PA, USA, 2020.

[15] International Organization for Standardization, *Biological Evaluation of Medical Devices—Part 23: Tests for Irritation*, ISO 10993-23:2021, Geneva, Switzerland, 2021.

[16] The World Bank Docs, “SELECTED INDICATORS*,” 2016. Accessed: Oct. 09, 2025. [Online]. Available:

<https://thedocs.worldbank.org/en/doc/b3502c65235d8c72aef5f34d87ed6298-0500062021/related/data-sen.pdf>

[17] ISO, ISO 13485:2016 – *Medical devices – Quality management systems – Requirements for regulatory purposes*, International Organization for Standardization, 2016. [Online]. Available:

<https://www.iso.org/standard/59752.html>

[18] ISO, ISO 14971:2019 – *Medical devices – Application of risk management to medical devices*, International Organization for Standardization, 2019. [Online]. Available:

<https://www.iso.org/standard/72704.html>

[19] ISO, ISO 10993-1:2018 – *Biological evaluation of medical devices – Part 1: Evaluation and testing within a risk management process*, International Organization for Standardization, 2018. [Online]. Available:

<https://www.iso.org/standard/68936.html>

[20] ISO, ISO 15223-1:2021 – *Medical devices – Symbols to be used with information to be supplied by the manufacturer – Part 1: General requirements*, International Organization for Standardization, 2021. [Online]. Available:

<https://www.iso.org/standard/78688.html>

[21] U.S. Food and Drug Administration, 21 CFR Part 820 – *Quality System Regulation*, U.S. Government Publishing Office, 2023. [Online]. Available:

<https://www.ecfr.gov/current/title-21/chapter-I/subchapter-H/part-820>

[22] “MPR Hand Traction System - MPR Orthopedics,” MPR Orthopedics, Nov. 22, 2022.

<https://mprortho.com/product/mpr-hand-traction-system> (accessed Sep. 17, 2025).

[23] “Equalizing Device shown with Finger Traps | David Scott Co,” Davidscottco.com, Jul. 11, 2024.

<https://www.davidscottco.com/product/equalizing-device-shown-with-finger-traps/> (accessed Sep. 17, 2025).

10.2 Mechanical Stand Fabrication Protocol

Description:

The aim is to ensure fabrication a mechanical body that meets the stability and adjustability requirements of the traction system. The mechanical body must be stable, height-adjustable, and compatible with clinical use. All components should remain durable under repeated loading and maintain structural integrity throughout orthopedic procedures.

Materials:

- Standard IV pole (height-adjustable)
- Aluminum sheet metal (for attachment platform)
- 3D-printed stoppers
- Bead chain segments
- D-rings

Additional Needed Items

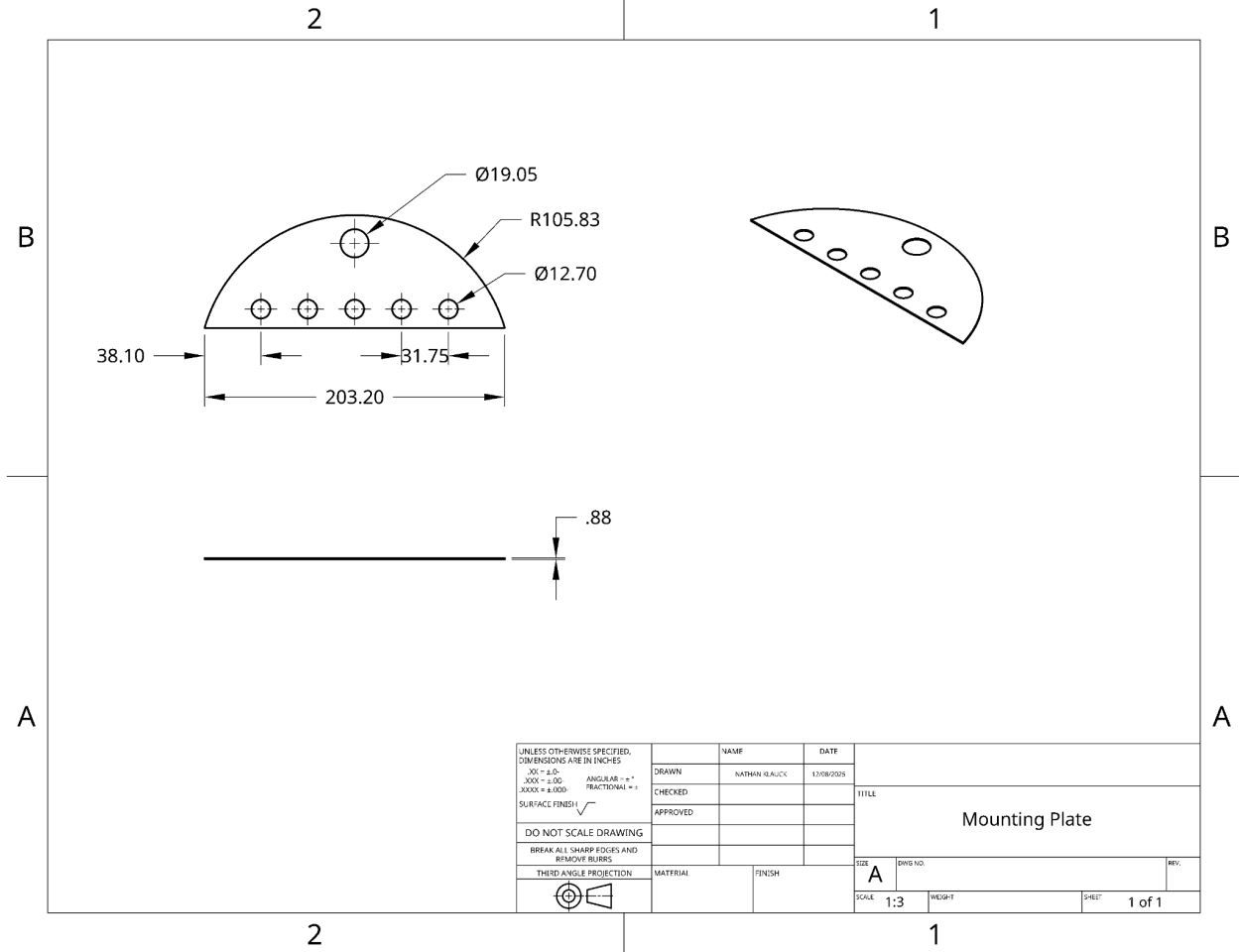
- Waterjet cutter
- Sandpaper or deburring tool
- Measuring tape or calipers
- Marker for layout lines
- 3D printer + filament for stopper components

Protocol:

1. Assembling the Medline Stand IV Pole
 - a. Unfold the base legs by spreading the four legs out from the center until the base is stable and flat on the ground. Make sure all legs are fully opened and resting evenly.
 - b. Assemble the central pole sections. The main pole comes in several pieces that must be inserted into one another in the correct order. Push or screw them together firmly so there are no gaps or instability present.
 - c. Once the sections are connected, loosen the collars around the central pole segments to extend the assembled body to the desired length. After you have adjusted, lock the collars on the central pole so the height is secure.
 - d. Once the pole has been made the desired height, secure the top-piece at the apex of the assembled pole.
2. Preparing the IV Pole Frame
 - a. Inspect the IV pole to ensure the height-adjustable central pole is firmly locked in place.
 - b. Remove any unnecessary parts (hooks/attachements) that interfere with mounting.
3. Cutting and Shaping the Mounting Plate
 - a. Design the desired component in CAD with precise dimensions to produce a file ready for cutting
 - b. Load the aluminum sheet into the waterjet cutter, ensuring it lies flat and is secured inside the machine.
 - c. Program and execute the waterjet cut following the design file for the platform.
 - d. Remove the cut piece and deburr sharp edges using sandpaper or a deburring tool.
4. Installing the 3D-Printed Stoppers

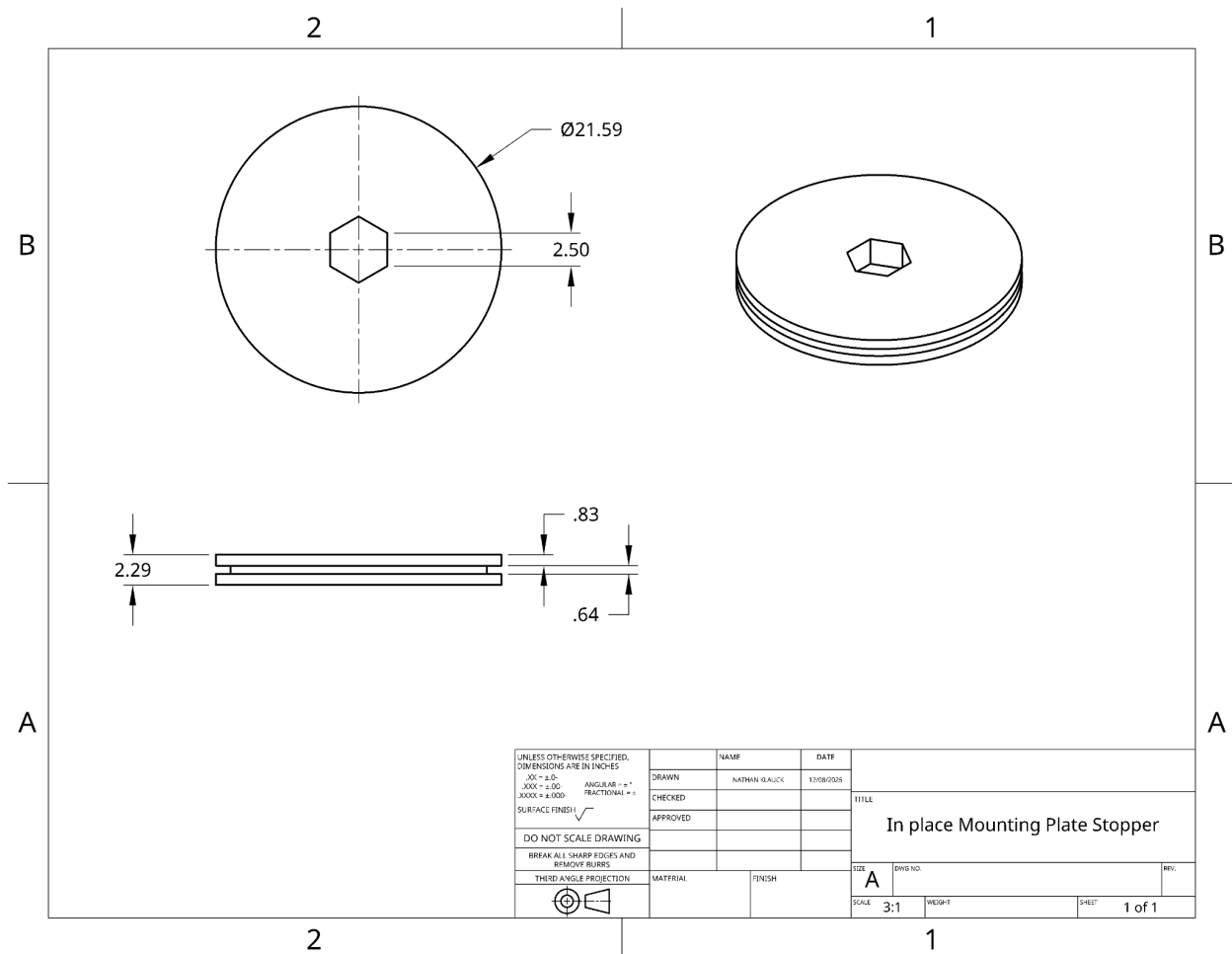
- a. Design the CAD drawing to 3-D print plate stopper
- 5. Full Assembly Inspection
 - a. Position the aluminum plate
 - b. Slide the 3D-printed stoppers onto the IV pole at the intended mounting height and confirm that the stopper prevents any rotational movement.
 - c. Connect bead-chain segments to the outer edges of the aluminum platform
 - d. Secure each chain with a bead-chain connector
 - e. Attach D-rings to the ends of the chains, ensuring they move freely and allow smooth traction adjustments.
- 6. Quality Check
 - a. Verify platform stability and alignment
 - b. Confirm that stoppers fully prevent slipping
 - c. Ensure bead-chain attachment points are secure
 - d. Inspect all edges for safe handling
 - e. Test full assembly under light simulated traction

10.3 Mounting Plate CAD Drawing



Note that the units listed for the CAD Drawing are all millimeters

10.4 In-place Mounting Plate Stopper CAD Drawing



Note that the units listed for the CAD Drawing are all millimeters

10.5 Finger Sleeve Fabrication Protocol

Description:

Our goal is to fabricate a reusable nylon finger sleeve that fits a range of finger sizes that aligns with our product designs specifications outlined in appendix 10.1 (Product Design Specification). This means that the sleeve must be compatible with autoclave sterilization and maintain its mechanical integrity after multiple uses. It should also be able to withstand tensile stresses up to 20 MPa.

Materials:

- Ballistic nylon fabric sheet
- Heavy duty nylon thread
- 1.5 cm D-ring
- Double sided velcro straps (12.7 x 10mm)

Additional Needed Items

- Laser cutter
- Sewing machine
- Fabric scissors
- Ruler or calipers
- Marking tool

Protocol:

1. Laser Cutting the Nylon Strips
 - a. Load ballistic nylon into the laser cutter and secure it to make sure it is flat
 - b. Program the cutter to create 5 strips measuring 44 x 1.5 cm using the laser cutter setting in the table below:

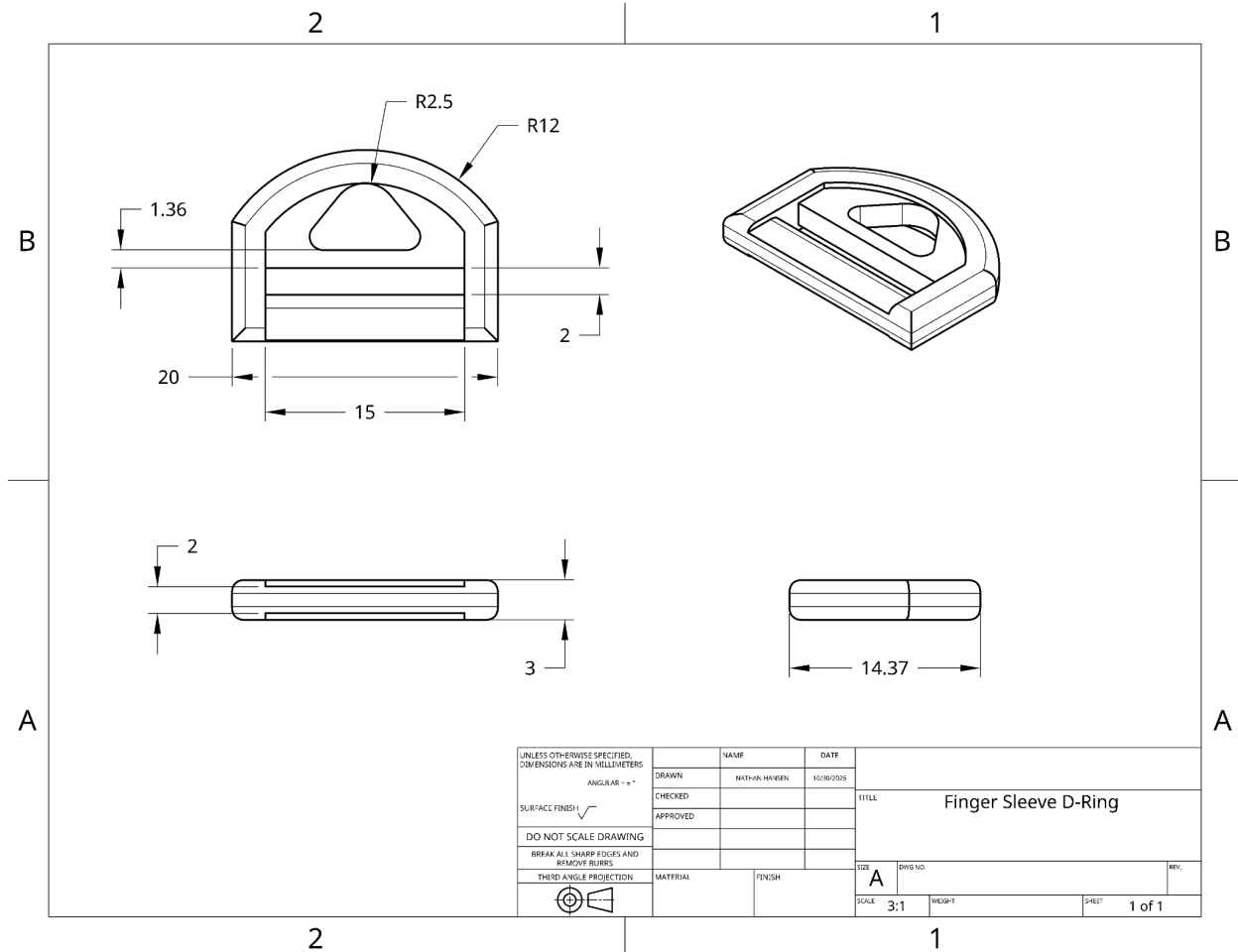
Table 1: Laser cutting settings used to create 5 ballistic nylon strips

Category	Parameter	Value
Material Info	Material Code	150002
	Watts	150 W
	Material Name	Ballistic Nylon
	Category	Fabric
Laser Mode	Mode	CO ₂ Parameters 10.6 um
Notes	Lens	2.0 lens
	Air Assist	Recommended
	Thickness	0.020"
Fiber Laser Settings	Simmer Power	2.00%
	Vector Cut Frequency	30 kHz
	Vector Cut Waveform	0
	Image Density	6
Vector Cutting - Red Pen	Density	300 PPI
	Max Cut Power	100%
	Max Cut Speed	90%
	Mid-point	0.000"
	Max Depth	0.000"

	Min Cut Speed	0.05%
	Data Entries	5

- c. Remove cut out strips from the template sheet
2. Forming the Sleeve Loop
 - a. Take a single 44 x 1.5 cm nylon strip
 - b. Overlap the two ends of the strip by 8 cm
 - i. Align edges cleanly for best stitching results
 - ii. Make sure it is untwisted
3. Stitching the Primary Seam
 - a. Using the sewing machine, apply a straight stitch running over the fabric 2-3 times back and forth across the overlapped 8 cm region
 - b. Trim any excess thread
4. Creating the Adjustable Slot Mechanism
 - a. Mark 5 evenly spaced slot lines spaced 1.6 cm apart on both sides of the loop
 - b. Stitch along the marked lines on each side, creating 5 slots on each side (10 total)
5. Adding the D Ring
 - a. Pass the long end of the loop through the 1.5 cm D ring
 - b. Pull enough of the nylon through to allow correct anchoring for the sleeve
6. Adding the Velcro Attachment System
 - a. Feed the first double sided velcro strip through the bottom most slot, for the base of the finger hold
 - b. Insert a second velcro strip through any of the remaining slots, depending on the finger length and girth
 - i. Note: you want the second strip to go on the body of the finger
7. Quality Check
 - a. Trim any extra stitching thread
 - b. Inspect for uniform slot spacing
 - c. Inspect for proper loop arrangement
 - d. Manually apply tension to confirm there is no premature deformation

10.6 Finger Sleeve D-Ring CAD Drawing



Note that the units listed for the CAD Drawing are all millimeters

10.7 Finite Element Analysis Testing Protocol

Description:

A testing protocol to determine whether the mounting plate is capable of withstanding the forces as outlined in Appendix 10.1 (Product Design Specification) without deformation.

Materials:

- SolidWorks FEA
- CAD of mounting plate

Protocol:

1. Import CAD file

2. Specify material as Aluminum 3003 Alloy
3. Start new FEA study
4. Fix model along top supporting hole
5. Apply bearing loads of 36 N along each of the 5 bottom weight bearing holes (simulating 45 N total with a FOS of 4)
6. Run study and look for areas of high stress or areas that exceed yield stress

10.8 Autoclaved Tensile Testing Protocol

Description:

A testing protocol to determine how much tensile force the finger sleeve can withstand before damage to the finger sleeve and before total failure of the finger sleeve. Additionally, the sleeve should maintain these strength properties after being autoclaved. This is important because the finger sleeve must be reusable and be able to withstand 20 MPa of tensile stress without damage.

Materials:

- 9 ballistic nylon dog bones
- Primus gravity autoclave
- 2 sterilization pouches
- MTS Insight - Model 5kN
- 1 kN load cell
- 100 N tensile grips
- Ruler

Protocol:

Autoclaving:

1. Place 6 out of the 9 dog bones into a sterilization pouch and put the pouch into the Primus autoclave
 - a. The other 3 dog bones can immediately be tensile tested
2. Run an hour long gravity cycle with a max temp of 251 °F (30 min sterilize, 30 min dry)
3. Pull the sterilization pouch out of the autoclave and allow it to reach room temperature
 - a. Check if the sterilization strip on the sterilization pouch has changed colors, indicating that the it has been properly sterilized
4. Remove 3 of the autoclaved dog bones from the sterilization pouch, these can be tensile tested
5. Transfer the other 3 autoclaved dog bones into a new sterilization pouch and put the pouch into the Primus autoclave
6. Run an hour long gravity cycle with a max temp of 251 °F (30 min sterilize, 30 min dry)
7. Pull the sterilization pouch out of the autoclave and allow it to reach room temperature
8. Repeat steps 6-7 three more times in the same sterilization bag so that the set of dog bones has been autoclaved 5 times
9. Conduct tensile testing on the last 3 dog bones

Tensile Testing:

1. Attach the 1 kN load cell and the 100 N tensile grips to the MTS Insight - Model 5kN system
2. Power on the TW Elite software and the MTS machine
3. Set the machine to tensile testing and change the test rate to 0.05 mm/s
4. Right click on load and zero the signal
5. Unlock the hand held machine control to be able to move the crosshead up
6. Secure the finger sleeve prototype between the tensile grips of the system, making sure the sleeve is aligned along the axis of tension to avoid uneven loading (pictured below)



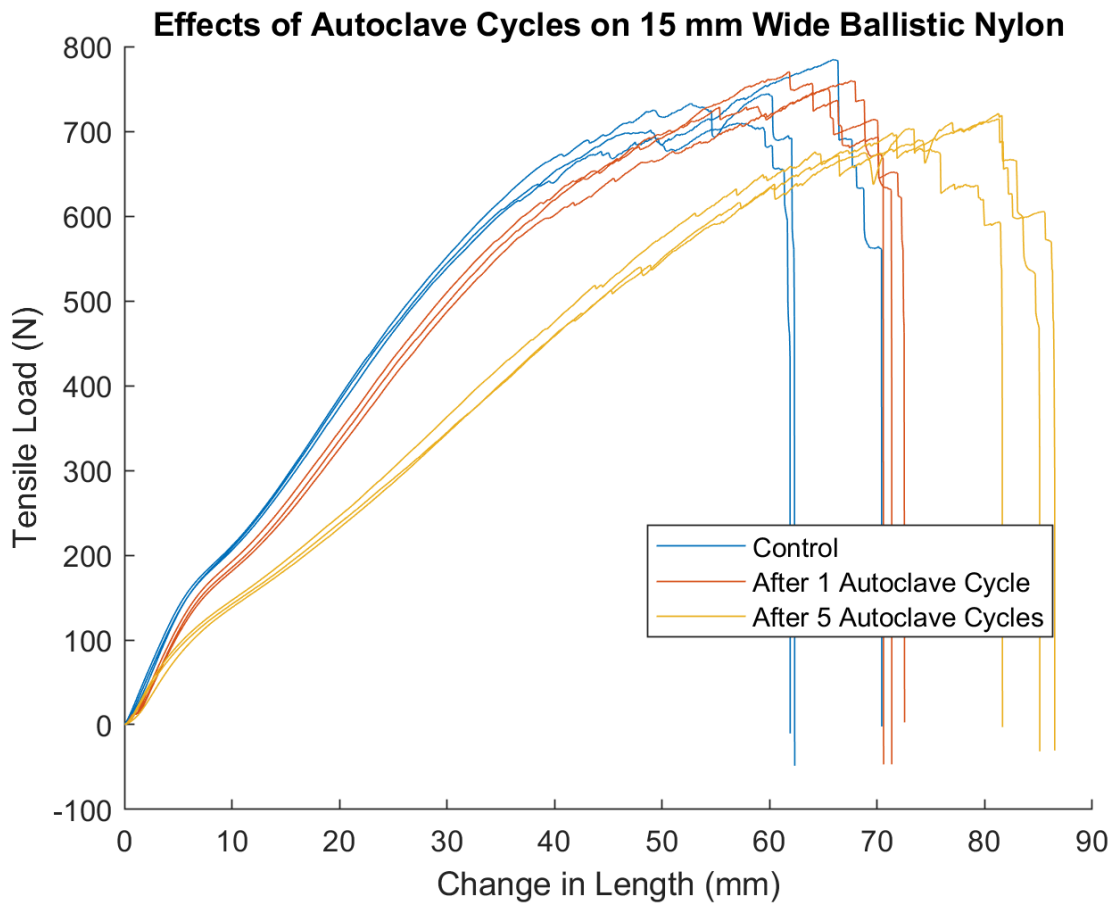
7. Set the initial grip separation to match the relaxed length of the finger sleeve (measured without tension) and record this starting length for strain calculations
8. Zero the load again and also click the crosshead box to zero it
9. Lock the hand held control
10. Begin running the MTS machine until it reaches a max force of 1 kN or until the material fails.
11. Right click on the data and export the raw data to a folder
12. Repeat this process for each ballistic nylon dog bone
13. Turn off the machine, close the software, return all components to their original storage area, and clean the MTS machine

10.9 Autoclaved Tensile Testing Raw MTS Data

[Control MTS data](#)

[MTS data after one autoclave cycle](#)

[MTS data after 5 autoclave cycles](#)



10.10 Autoclaved Tensile Testing MATLAB Code

%% Import Data

```
control1 = "C:\Users\Nathan\OneDrive\Ballistic Nylon Testing\Control\DAQ- Crosshead, ... - (Timed) (0).txt";
control2 = "C:\Users\Nathan\OneDrive\Ballistic Nylon Testing\Control\DAQ- Crosshead, ... - (Timed) (1).txt";
control3 = "C:\Users\Nathan\OneDrive\Ballistic Nylon Testing\Control\DAQ- Crosshead, ... - (Timed) (2).txt";
C1normal1 = "C:\Users\Nathan\OneDrive\Ballistic Nylon Testing\1 Cycle (normal)\DAQ- Crosshead, ... - (Timed) (6).txt";
C1normal2 = "C:\Users\Nathan\OneDrive\Ballistic Nylon Testing\1 Cycle (normal)\DAQ- Crosshead, ... - (Timed) (7).txt";
C1normal3 = "C:\Users\Nathan\OneDrive\Ballistic Nylon Testing\1 Cycle (normal)\DAQ- Crosshead, ... - (Timed) (8).txt";
C5normal1 = "C:\Users\Nathan\OneDrive\Ballistic Nylon Testing\5 Cycles (stitches)\DAQ- Crosshead, ... - (Timed) (12).txt";
C5normal2 = "C:\Users\Nathan\OneDrive\Ballistic Nylon Testing\5 Cycles (stitches)\DAQ- Crosshead, ... - (Timed) (13).txt";
C5normal3 = "C:\Users\Nathan\OneDrive\Ballistic Nylon Testing\5 Cycles (stitches)\DAQ- Crosshead, ... - (Timed) (14).txt";
c1 = readtable(control1, detectImportOptions(control1, 'NumHeaderLines', 4));
c2 = readtable(control2, detectImportOptions(control2, 'NumHeaderLines', 4));
c3 = readtable(control3, detectImportOptions(control3, 'NumHeaderLines', 4));
n1c1 = readtable(C1normal1, detectImportOptions(C1normal1, 'NumHeaderLines', 4));
n2c1 = readtable(C1normal2, detectImportOptions(C1normal2, 'NumHeaderLines', 4));
n3c1 = readtable(C1normal3, detectImportOptions(C1normal3, 'NumHeaderLines', 4));
n1c5 = readtable(C5normal1, detectImportOptions(C5normal1, 'NumHeaderLines', 4));
n2c5 = readtable(C5normal2, detectImportOptions(C5normal2, 'NumHeaderLines', 4));
n3c5 = readtable(C5normal3, detectImportOptions(C5normal3, 'NumHeaderLines', 4));
```

%% Extract each column

```

c1_crosshead = c1{:,1}; % mm
c1_load = c1{:,2}; % N
c1_time = c1{:,3}; % sec
c1_stress = c1_load ./ 6; % N/mm^2 or MPa
c1_strain = c1_crosshead ./ 135; % [-]
c2_crosshead = c2{:,1};
c2_load = c2{:,2};
c2_time = c2{:,3};
c2_stress = c2_load ./ 6;
c2_strain = c2_crosshead ./ 135;
c3_crosshead = c3{:,1};
c3_load = c3{:,2};
c3_time = c3{:,3};
c3_stress = c3_load ./ 6;
c3_strain = c3_crosshead ./ 135;
n1c1_crosshead = n1c1{:,1};
n1c1_load = n1c1{:,2};
n1c1_time = n1c1{:,3};
n1c1_stress = n1c1_load ./ 6;
n1c1_strain = n1c1_crosshead ./ 135;
n2c1_crosshead = n2c1{:,1};
n2c1_load = n2c1{:,2};
n2c1_time = n2c1{:,3};
n2c1_stress = n2c1_load ./ 6;
n2c1_strain = n2c1_crosshead ./ 135;
n3c1_crosshead = n3c1{:,1};
n3c1_load = n3c1{:,2};
n3c1_time = n3c1{:,3};
n3c1_stress = n3c1_load ./ 6;
n3c1_strain = n3c1_crosshead ./ 135;
n1c5_crosshead = n1c5{:,1};
n1c5_load = n1c5{:,2};
n1c5_time = n1c5{:,3};
n1c5_stress = n1c5_load ./ 6;
n1c5_strain = n1c5_crosshead ./ 125;
n2c5_crosshead = n2c5{:,1};
n2c5_load = n2c5{:,2};
n2c5_time = n2c5{:,3};
n2c5_stress = n2c5_load ./ 6;
n2c5_strain = n2c5_crosshead ./ 125;
n3c5_crosshead = n3c5{:,1};
n3c5_load = n3c5{:,2};
n3c5_time = n3c5{:,3};
n3c5_stress = n3c5_load ./ 6;
n3c5_strain = n3c5_crosshead ./ 125;
%% Plotting Stress vs. Strain
figure (2)
hold on
h1 = plot(c1_strain, c1_stress, 'Color', blue);
plot(c2_strain, c2_stress, 'Color', blue)
plot(c3_strain, c3_stress, 'Color', blue)
h2 = plot(n1c1_strain, n1c1_stress, 'Color', red);
plot(n2c1_strain, n2c1_stress, 'Color', red)
plot(n3c1_strain, n3c1_stress, 'Color', red)

```



```

h3 = plot(n1c5_strain, n1c5_stress, 'Color', gold);
plot(n2c5_strain, n2c5_stress, 'Color', gold)
plot(n3c5_strain, n3c5_stress, 'Color', gold)
title("Stress Strain Curve of Ballistic Nylon Before and After Autoclave Cycles")
xlabel("Strain [-]")
ylabel("Stress (MPa)")
legend([h1 h2 h3], {'Control', 'After 1 Autoclave Cycle', 'After 5 Autoclave Cycles'}, 'Location', 'best');
hold off

%%% Independent Single-Tailed T-test Maximum Load (Control & 1 Cycle)
control_load_max = [
    max(c1_load)
    max(c2_load)
    max(c3_load)
];
autoclave1_load_max = [
    max(n1c1_load)
    max(n2c1_load)
    max(n3c1_load)
];
[h_load_cto1, p_load_cto1] = ttest2(control_load_max, autoclave1_load_max, 'Tail', 'left') % h=0, p=0.2844
%%% Independent Single-Tailed T-test Maximum Stress (Control & 1 Cycle)
control_stress_max = [
    max(c1_stress)
    max(c2_stress)
    max(c3_stress)
];
autoclave1_stress_max = [
    max(n1c1_stress)
    max(n2c1_stress)
    max(n3c1_stress)
];
[h_stress_cto1, p_stress_cto1] = ttest2(control_stress_max, autoclave1_stress_max, 'Tail', 'left') % h=0, p=0.2844
%%% Independent 2-Tailed T-test Elastic Modulus (Control & 1 Cycle)
lower = 0.10;
upper = 0.20;
idx_c1 = c1_strain >= lower & c1_strain <= upper;
idx_c2 = c2_strain >= lower & c2_strain <= upper;
idx_c3 = c3_strain >= lower & c3_strain <= upper;
idx_n1 = n1c1_strain >= lower & n1c1_strain <= upper;
idx_n2 = n2c1_strain >= lower & n2c1_strain <= upper;
idx_n3 = n3c1_strain >= lower & n3c1_strain <= upper;
control_modulus = [
    polyfit(c1_strain(idx_c1), c1_stress(idx_c1), 1);
    polyfit(c2_strain(idx_c2), c2_stress(idx_c2), 1);
    polyfit(c3_strain(idx_c3), c3_stress(idx_c3), 1);
];
autoclave1_modulus = [
    polyfit(n1c1_strain(idx_n1), n1c1_stress(idx_n1), 1);
    polyfit(n2c1_strain(idx_n2), n2c1_stress(idx_n2), 1);
    polyfit(n3c1_strain(idx_n3), n3c1_stress(idx_n3), 1);
];
control_E = control_modulus(:,1);
autoclave1_E = autoclave1_modulus(:,1);
[h_mod_cto1, p_mod_cto1] = ttest2(control_E, autoclave1_E) % h=1, p=0.0038

```

```

%%% Independent 2-Tailed T-test Failure Strain (Control & 1 Cycle)
control_failure_strain = [
    max(c1_strain)
    max(c2_strain)
    max(c3_strain)
];
autoclave1_failure_strain = [
    max(n1c1_strain)
    max(n2c1_strain)
    max(n3c1_strain)
];
[h_strain_cto1, p_strain_cto1] = ttest2(control_failure_strain, autoclave1_failure_strain) % h=0, p=0.0796
%%% Independent Single-Tailed T-test Maximum Stress (Control & 5 Cycle)
control_stress_max = [
    max(c1_stress)
    max(c2_stress)
    max(c3_stress)
];
autoclave5_stress_max = [
    max(n1c5_stress)
    max(n2c5_stress)
    max(n3c5_stress)
];
[h_stress_cto5, p_stress_cto5] = ttest2(control_stress_max, autoclave5_stress_max, 'Tail', 'right') % h=0, p=0.1049
%%% Independent 2-Tailed T-test Elastic Modulus (Control & 5 Cycle)
lower = 0.10;
upper = 0.20;
idx_c1 = c1_strain >= lower & c1_strain <= upper;
idx_c2 = c2_strain >= lower & c2_strain <= upper;
idx_c3 = c3_strain >= lower & c3_strain <= upper;
idx_n1 = n1c5_strain >= lower & n1c5_strain <= upper;
idx_n2 = n2c5_strain >= lower & n2c5_strain <= upper;
idx_n3 = n3c5_strain >= lower & n3c5_strain <= upper;
control_modulus = [
    polyfit(c1_strain(idx_c1), c1_stress(idx_c1), 1);
    polyfit(c2_strain(idx_c2), c2_stress(idx_c2), 1);
    polyfit(c3_strain(idx_c3), c3_stress(idx_c3), 1);
];
autoclave5_modulus = [
    polyfit(n1c5_strain(idx_n1), n1c5_stress(idx_n1), 1);
    polyfit(n2c5_strain(idx_n2), n2c5_stress(idx_n2), 1);
    polyfit(n3c5_strain(idx_n3), n3c5_stress(idx_n3), 1);
];
control_E = control_modulus(:,1);
autoclave5_E = autoclave5_modulus(:,1);
[h_mod_cto5, p_mod_cto5] = ttest2(control_E, autoclave5_E) % h=1, p=2.2950e-06
%%% Independent 2-Tailed T-test Failure Strain (Control & 5 Cycle)
control_failure_strain = [
    max(c1_strain)
    max(c2_strain)
    max(c3_strain)
];
autoclave5_failure_strain = [
    max(n1c5_strain)

```

```

max(n2c5_strain)
max(n3c5_strain)
];
[h_strain_cto5, p_strain_cto5] = ttest2(control_failure_strain, autoclave5_failure_strain) % h=1, p=0.0012
%%% Independent Single-Tailed T-test Maximum Stress (1 Cycle & 5 Cycle)
autoclave1_stress_max = [
    max(n1c1_stress)
    max(n2c1_stress)
    max(n3c1_stress)
];
autoclave5_stress_max = [
    max(n1c5_stress)
    max(n2c5_stress)
    max(n3c5_stress)
];
[h_stress_1to5, p_stress_1to5] = ttest2(autoclave1_stress_max, autoclave5_stress_max, 'Tail', 'right') % h=1, p=0.0018
%%% Independent 2-Tailed T-test Elastic Modulus (1 Cycle & 5 Cycle)
lower = 0.10;
upper = 0.20;
idx_c1 = n1c1_strain >= lower & n1c1_strain <= upper;
idx_c2 = n2c1_strain >= lower & n2c1_strain <= upper;
idx_c3 = n3c1_strain >= lower & n3c1_strain <= upper;
idx_n1 = n1c5_strain >= lower & n1c5_strain <= upper;
idx_n2 = n2c5_strain >= lower & n2c5_strain <= upper;
idx_n3 = n3c5_strain >= lower & n3c5_strain <= upper;
autoclave1_modulus = [
    polyfit(n1c1_strain(idx_c1), n1c1_stress(idx_c1), 1);
    polyfit(n2c1_strain(idx_c2), n2c1_stress(idx_c2), 1);
    polyfit(n3c1_strain(idx_c3), n3c1_stress(idx_c3), 1);
];
autoclave5_modulus = [
    polyfit(n1c5_strain(idx_n1), n1c5_stress(idx_n1), 1);
    polyfit(n2c5_strain(idx_n2), n2c5_stress(idx_n2), 1);
    polyfit(n3c5_strain(idx_n3), n3c5_stress(idx_n3), 1);
];
autoclave1_E = autoclave1_modulus(:,1);
autoclave5_E = autoclave5_modulus(:,1);
[h_mod_1to5, p_mod_1to5] = ttest2(autoclave1_E, autoclave5_E) % h=1, p=8.2444e-06
%%% Independent 2-Tailed T-test Failure Strain (1 Cycle & 5 Cycle)
autoclave1_failure_strain = [
    max(n1c1_strain)
    max(n2c1_strain)
    max(n3c1_strain)
];
autoclave5_failure_strain = [
    max(n1c5_strain)
    max(n2c5_strain)
    max(n3c5_strain)
];
[h_strain_1to5, p_strain_1to5] = ttest2(autoclave1_failure_strain, autoclave5_failure_strain) % h=1, p=0.2.9005e-04
%%% Stress Box Plot
data = [control_stress_max; autoclave1_stress_max; autoclave5_stress_max];
group = [repmat("Control", length(control_stress_max),1);
    repmat("1 Cycle", length(autoclave1_stress_max),1);

```

```

        repmat("5 Cycles", length(autoclave5_stress_max),1)];
figure (4);
boxplot(data, group, 'Symbol', 'o');
ylabel("Maximum Stress (MPa)");
title("Comparison of Maximum Stress After Autoclave Cycles");
set(gca, 'FontSize', 12);
ylim([115 140])
hold on;
% === APPLY COLORS ===
h = findobj(gca, 'Tag', 'Box');
colors = {gold, red, blue};
% Box order returned: 5 cycles, 1 cycle, control
for i = 1:length(h)
    patch(get(h(i), 'XData'), get(h(i), 'YData'), colors{i}, ...
        'FaceAlpha', 0.4, 'EdgeColor', colors{i}, 'LineWidth', 1.5);
end
% --- Convert p-values to symbols ---
sig_cto1 = sigStar(p_stress_cto1);
sig_cto5 = sigStar(p_stress_cto5);
sig_1to5 = sigStar(p_stress_1to5);
% --- Draw brackets ---
ymax = max(data) * 0.84;
if sig_cto1 ~= ""
    drawBracket(1, 2, ymax, sig_cto1);
end
if sig_cto5 ~= ""
    drawBracket(1, 3, ymax*1.10, sig_cto5);
end
if sig_1to5 ~= ""
    drawBracket(2, 3, ymax*1.20, sig_1to5);
end
hold off;
function s = sigStar(p)
    if p < 0.01
        s = "***";
    elseif p < 0.05
        s = "**";
    else
        s = "";
    end
end
function drawBracket(x1, x2, y, labelText)
    plot([x1 x1 x2 x2], [y y+0.02*y y+0.02*y y], 'k', 'LineWidth', 1.5);
    text(mean([x1 x2]), y + 0.03*y, labelText, ...
        'HorizontalAlignment', 'center', 'FontSize', 14);
end
%% Elastic Modulus Box Plot
data = [control_E; autoclave1_E; autoclave5_E];
group = [repmat("Control", length(control_E),1);
    repmat("1 Cycle", length(autoclave1_E),1);
    repmat("5 Cycles", length(autoclave5_E),1)];
figure (5);
boxplot(data, group, 'Symbol', 'o');
ylabel("Elastic Modulus (MPa)");

```

```

title("Comparison of Elastic Modulus After Autoclave Cycles");
set(gca, 'FontSize', 12);
ylim([190 475]) % adjust as needed based on your modulus values
hold on;
% === APPLY COLORS ===
h = findobj(gca, 'Tag', 'Box');
colors = {gold, red, blue}; % Box order returned: 5 cycles, 1 cycle, control
for i = 1:length(h)
    patch(get(h(i), 'XData'), get(h(i), 'YData'), colors{i}, ...
        'FaceAlpha', 0.4, 'EdgeColor', colors{i}, 'LineWidth', 1.5);
end
% --- Convert p-values to symbols ---
sig_cto1 = sigStar(p_mod_cto1);
sig_cto5 = sigStar(p_mod_cto5);
sig_1to5 = sigStar(p_mod_1to5);
% --- Draw brackets ---
ymax = max(data) * 1.02;
if sig_cto1 ~= ""
    drawBracket(1, 2, ymax, sig_cto1);
end
if sig_cto5 ~= ""
    drawBracket(1, 3, ymax*1.05, sig_cto5);
end
if sig_1to5 ~= ""
    drawBracket(2, 3, ymax, sig_1to5);
end
hold off;
%% Failure Strain Box Plot
data = [control_failure_strain; autoclave1_failure_strain; autoclave5_failure_strain];
group = [repmat("Control", length(control_failure_strain), 1);
    repmat("1 Cycle", length(autoclave1_failure_strain), 1);
    repmat("5 Cycles", length(autoclave5_failure_strain), 1)];
figure(6);
boxplot(data, group, 'Symbol', 'o');
ylabel("Failure Strain [-]");
title("Comparison of Failure Strain After Autoclave Cycles");
set(gca, 'FontSize', 12);
ylim([0.4 0.8]); % adjust based on your actual strain values
hold on;
% === APPLY COLORS ===
h = findobj(gca, 'Tag', 'Box');
colors = {gold, red, blue}; % Box order returned: 5 cycles, 1 cycle, control
for i = 1:length(h)
    patch(get(h(i), 'XData'), get(h(i), 'YData'), colors{i}, ...
        'FaceAlpha', 0.4, 'EdgeColor', colors{i}, 'LineWidth', 1.5);
end
% --- Convert p-values to symbols ---
sig_cto1 = sigStar(p_strain_cto1);
sig_cto5 = sigStar(p_strain_cto5);
sig_1to5 = sigStar(p_strain_1to5);
% --- Draw brackets ---
ymax = max(data) * 1.02;
if sig_cto1 ~= ""
    drawBracket(1, 2, ymax, sig_cto1);

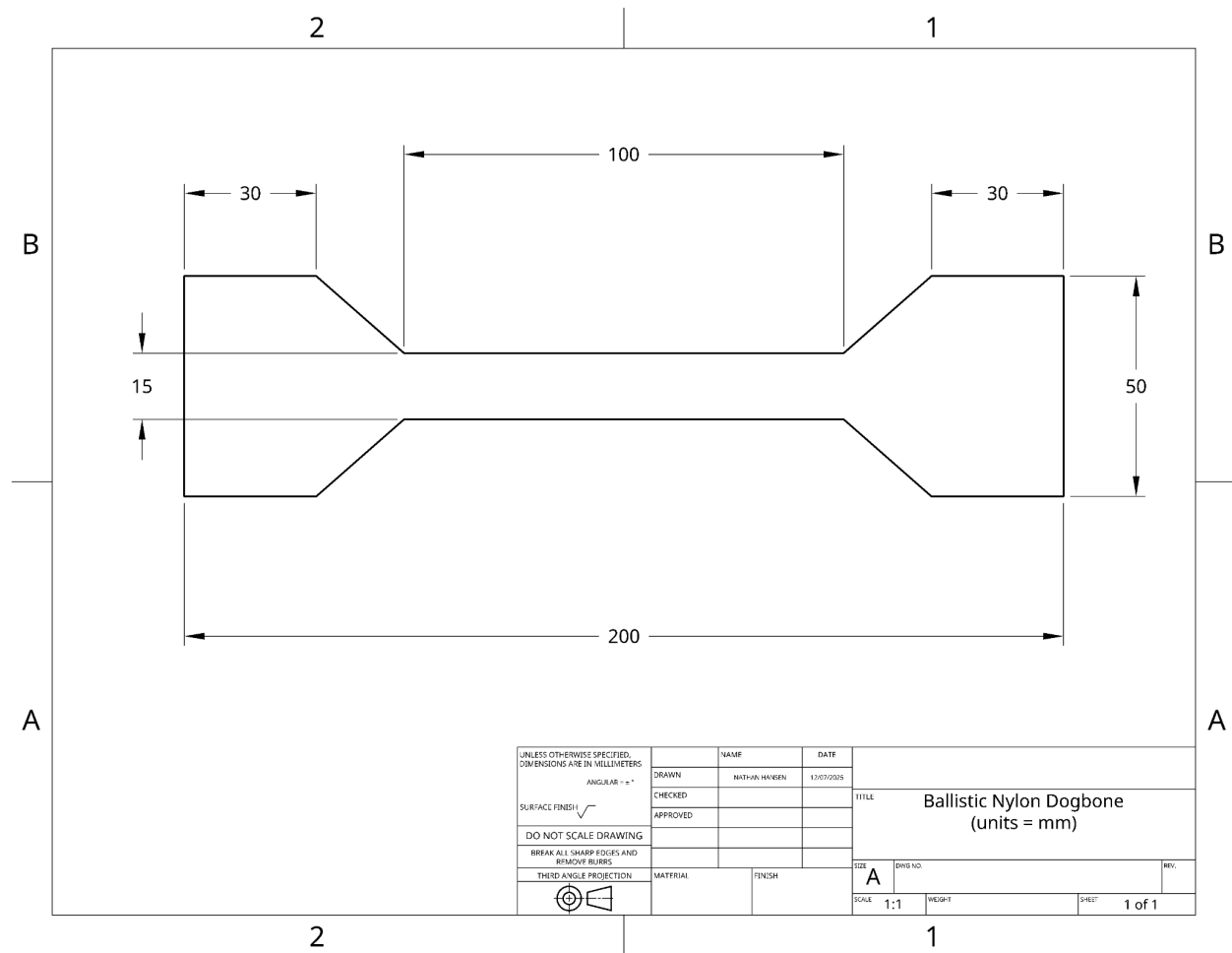
```

```

end
if sig_cto5 ~= ""
    drawBracket(1, 3, ymax*1.05, sig_cto5);
end
if sig_lto5 ~= ""
    drawBracket(2, 3, ymax, sig_lto5);
end
hold off;

```

10.11 Dog Bone CAD Drawing



10.12 Slippage Testing Protocol

Description:

A testing protocol to determine how much the finger sleeve will slip on the average finger, so that the finger sleeves can be used for 50 minute operations without the risk of the finger sleeve losing grip of the finger.

Materials:

- Prototype of finger sleeve
- Stop watch
- Caliper
- Willing Participants
- Wooden Board
- Nail in which sleeve will hang
- Permanent marker

Protocol:

1. Take the nail and hammer it into the ply board to act as a hook
2. Have the participant sit in the chair and attach the finger sleeve to the stand, having the participant hang their arm from the stand with their shoulder and elbow at a 90 degree angle
 - a. Make sure that the participants arm is not resting on the chair and that the forearm is hanging perpendicular to the floor
3. Properly secure the finger sleeve prototype to one of the participants fingers and mark the initial pretested point
4. Once, the participant is in the proper position, start the stopwatch
5. Wait for the timer to reach 10 minutes, and then make a mark on the finger of the participant, after the dot is created the sleeve can be disconnected and the participant can relax their arm
6. Using the caliper, measure the distance in mm to the nearest tenth between the first mark and the second.
7. Repeat this process for each participants finger

10.13 Slippage Testing Raw Data

Finger	Person	Proximal Displacement	Middle Displacement	Length	Girth
Pointer	P1	1.5 mm	2.2 mm	95 mm	60 mm
	P2	0.0 mm	2.0 mm	83 mm	52 mm
Middle	P1	1.2 mm	0.0 mm	109 mm	65 mm
	P2	0.8 mm	1.5 mm	98 mm	61 mm
Ring	P1	0.0 mm	1.5 mm	98 mm	58 mm
	P2	1.3 mm	0.0 mm	90 mm	54 mm
Pinky	P1	2.0 mm	0.0 mm	62 mm	48 mm
	P2	1.5 mm	1.1 mm	60 mm	42 mm

10.14 Stitched Tensile Testing Protocol

Description:

A testing protocol to determine how much tensile force the stitching of the finger sleeve can withstand before damage to the finger sleeve and before total failure of the finger sleeve. Additionally, the stitching should maintain these strength properties after being autoclaved. This is important because the finger sleeve must be reusable and be able to withstand 20 MPa of tensile stress without damage.

Materials:

- 6 ballistic nylon dog bones
- Sewing machine
- Medium size thread
- Primus gravity autoclave
- 2 sterilization pouches
- MTS Insight - Model 5kN
- 1 kN load cell
- 100 N tensile grips
- Ruler

Protocol:

Stitching:

1. Using a pair of scissors, cut the dog bone in half across the 15 mm wide section
2. Overlap the two ends of each half by 10 mm and using the sewing machine, apply a straight stitch running over the fabric 2-3 times back and forth across in the middle of the overlay
3. Repeat these steps for each ballistic nylon dog bone

Autoclaving:

1. Place 3 out of the 6 stitched dog bones into a sterilization pouch and put the pouch into the Primus autoclave
 - a. The other 3 dog bones can immediately be tensile tested
2. Run an hour long gravity cycle with a max temp of 251 °F (30 min sterilize, 30 min dry)
3. Pull the sterilization pouch out of the autoclave and allow it to reach room temperature
 - a. Check if the sterilization strip on the sterilization pouch has changed colors, indicating that it has been properly sterilized
4. Conduct tensile testing on the last 3 dog bones

Tensile Testing:

1. Attach the 1 kN load cell and the 100 N tensile grips to the MTS Insight - Model 5kN system
2. Power on the TW Elite software and the MTS machine
3. Set the machine to tensile testing and change the test rate to 0.05 mm/s
4. Right click on load and zero the signal
5. Unlock the hand held machine control to be able to move the crosshead up

6. Secure the finger sleeve prototype between the tensile grips of the system, making sure the sleeve is aligned along the axis of tension to avoid uneven loading (pictured below)

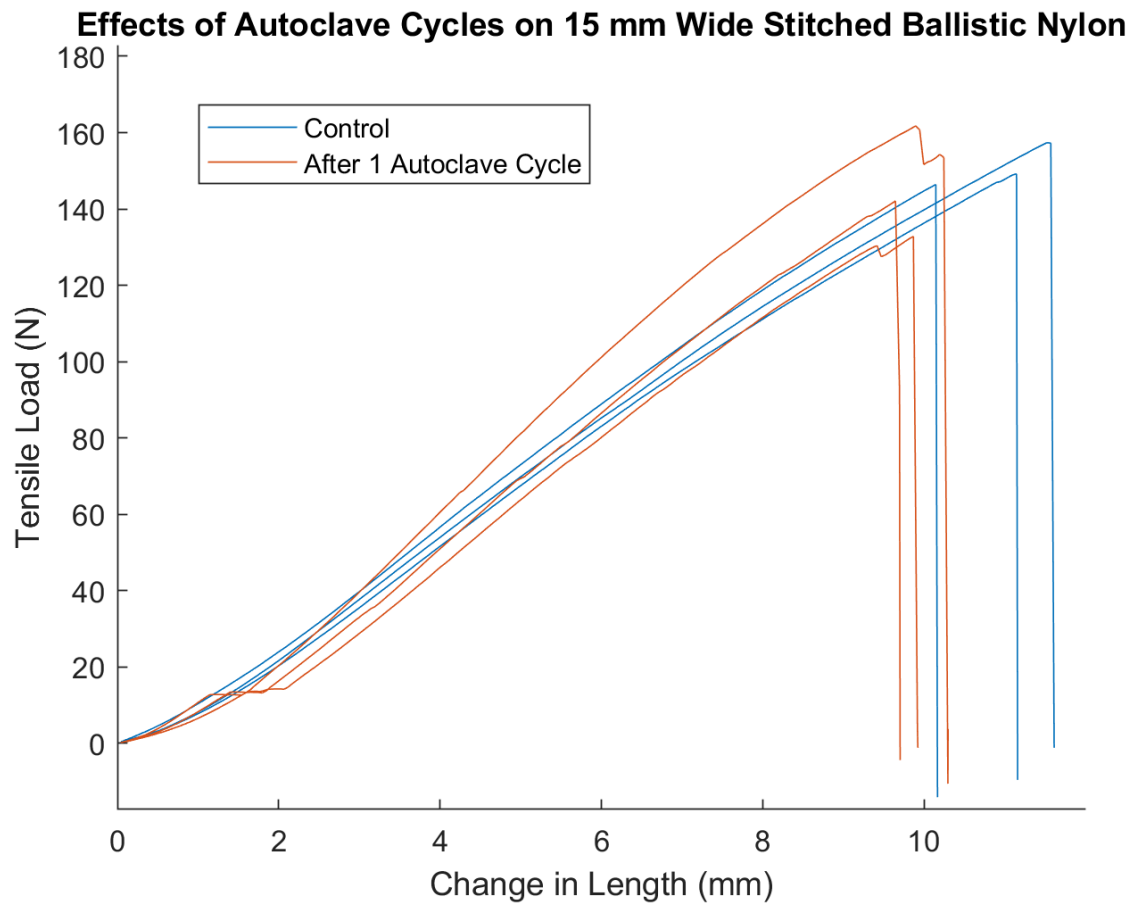


7. Set the initial grip separation to match the relaxed length of the finger sleeve (measured without tension) and record this starting length for strain calculations
8. Zero the load again and also click the crosshead box to zero it
9. Lock the hand held control
10. Begin running the MTS machine until it reaches a max force of 1 kN or until the material fails.
11. Right click on the data and export the raw data to a folder
12. Repeat this process for each ballistic nylon dog bone
13. Turn off the machine, close the software, return all components to their original storage area, and clean the MTS machine

10.15 Stitched Tensile Testing Raw MTS Data

[Stitched control MTS data](#)

[Stitched MTS data after one autoclave cycle](#)



10.16 Stitched Tensile Testing MATLAB Code

```
%% Import Data
stitchesC1 = "C:\Users\Nathan\OneDrive\Ballistic Nylon Testing\Stitches Control\DAQ- Crosshead, ... - (Timed) (3).txt";
stitchesC2 = "C:\Users\Nathan\OneDrive\Ballistic Nylon Testing\Stitches Control\DAQ- Crosshead, ... - (Timed) (4).txt";
stitchesC3 = "C:\Users\Nathan\OneDrive\Ballistic Nylon Testing\Stitches Control\DAQ- Crosshead, ... - (Timed) (5).txt";
C1stitches1 = "C:\Users\Nathan\OneDrive\Ballistic Nylon Testing\1 Cycle (stitches)\DAQ- Crosshead, ... - (Timed) (9).txt";
C1stitches2 = "C:\Users\Nathan\OneDrive\Ballistic Nylon Testing\1 Cycle (stitches)\DAQ- Crosshead, ... - (Timed) (10).txt";
C1stitches3 = "C:\Users\Nathan\OneDrive\Ballistic Nylon Testing\1 Cycle (stitches)\DAQ- Crosshead, ... - (Timed) (11).txt";
s1 = readtable(stitchesC1, detectImportOptions(stitchesC1, 'NumHeaderLines', 4));
s2 = readtable(stitchesC2, detectImportOptions(stitchesC2, 'NumHeaderLines', 4));
s3 = readtable(stitchesC3, detectImportOptions(stitchesC3, 'NumHeaderLines', 4));
s1c1 = readtable(C1stitches1, detectImportOptions(C1stitches1, 'NumHeaderLines', 4));
s2c1 = readtable(C1stitches2, detectImportOptions(C1stitches2, 'NumHeaderLines', 4));
s3c1 = readtable(C1stitches3, detectImportOptions(C1stitches3, 'NumHeaderLines', 4));
%% Extract each column
s1_crosshead = s1{:,1};
s1_load = s1{:,2};
s1_time = s1{:,3};
s1_stress = s1_load ./ 6;
s1_strain = s1_crosshead ./ 125;
s2_crosshead = s2{:,1};
s2_load = s2{:,2};
```

```

s2_time = s2{:,3};
s2_stress = s2_load ./ 6;
s2_strain = s2_crosshead ./ 125;
s3_crosshead = s3{:,1};
s3_load = s3{:,2};
s3_time = s3{:,3};
s3_stress = s3_load ./ 6;
s3_strain = s3_crosshead ./ 125;
s1c1_crosshead = s1c1{:,1};
s1c1_load = s1c1{:,2};
s1c1_time = s1c1{:,3};
s1c1_stress = s1c1_load ./ 6;
s1c1_strain = s1c1_crosshead ./ 125;
s2c1_crosshead = s2c1{:,1};
s2c1_load = s2c1{:,2};
s2c1_time = s2c1{:,3};
s2c1_stress = s2c1_load ./ 6;
s2c1_strain = s2c1_crosshead ./ 125;
s3c1_crosshead = s3c1{:,1};
s3c1_load = s3c1{:,2};
s3c1_time = s3c1{:,3};
s3c1_stress = s3c1_load ./ 6;
s3c1_strain = s3c1_crosshead ./ 125;
n1c5_crosshead = n1c5{:,1};
%% Plotting Stress vs. Strain (stitches)
figure(3)
hold on
h1 = plot(s1_strain, s1_stress, 'Color', blue);
plot(s2_strain, s2_stress, 'Color', blue)
plot(s3_strain, s3_stress, 'Color', blue)
h2 = plot(s1c1_strain, s1c1_stress, 'Color', red);
plot(s2c1_strain, s2c1_stress, 'Color', red)
plot(s3c1_strain, s3c1_stress, 'Color', red)
title("Stress Strain Curve of Stitched Ballistic Nylon Before and After One Autoclave Cycle")
xlabel("Strain [-]")
ylabel("Stress (MPa)")
legend([h1 h2], {'Control', 'After 1 Autoclave Cycle'}, 'Location', 'best');
hold off
%% Independent Single-Tailed T-test Maximum Stress (Stitches)
control_sti_stress_max = [
    max(s1_stress)
    max(s2_stress)
    max(s3_stress)
];
autoclave_sti_stress_max = [
    max(s1c1_stress)
    max(s2c1_stress)
    max(s3c1_stress)
];
[h_stress_sti, p_stress_sti] = ttest2(control_sti_stress_max, autoclave_sti_stress_max, 'Tail', 'right') % h=0, p=0.2923
%% Independent 2-Tailed T-test Elastic Modulus (Stitches)
lower = 0.02;
upper = 0.05;
idx_s1 = s1_strain >= lower & s1_strain <= upper;

```

```

idx_s2 = s2_strain >= lower & s2_strain <= upper;
idx_s3 = s3_strain >= lower & s3_strain <= upper;
idx_s1c1 = s1c1_strain >= lower & s1c1_strain <= upper;
idx_s2c1 = s2c1_strain >= lower & s2c1_strain <= upper;
idx_s3c1 = s3c1_strain >= lower & s3c1_strain <= upper;
control_sti_modulus = [
    polyfit(s1_strain(idx_s1), s1_stress(idx_s1), 1);
    polyfit(s2_strain(idx_s2), s2_stress(idx_s2), 1);
    polyfit(s3_strain(idx_s3), s3_stress(idx_s3), 1);
];
autoclave_sti_modulus = [
    polyfit(s1c1_strain(idx_s1c1), s1c1_stress(idx_s1c1), 1);
    polyfit(s2c1_strain(idx_s2c1), s2c1_stress(idx_s2c1), 1);
    polyfit(s3c1_strain(idx_s3c1), s3c1_stress(idx_s3c1), 1);
];
control_sti_E = control_sti_modulus(:,1);
autoclave_sti_E = autoclave_sti_modulus(:,1);
[h_mod_sti, p_mod_sti] = ttest2(control_sti_E, autoclave_sti_E) % h=0, p=0.0698
%%% Independent 2-Tailed T-test Failure Strain (Stitches)
control_sti_failure_strain = [
    max(s1_strain)
    max(s2_strain)
    max(s3_strain)
];
autoclave_sti_failure_strain = [
    max(s1c1_strain)
    max(s2c1_strain)
    max(s3c1_strain)
];
[h_strain_sti, p_strain_sti] = ttest2(control_sti_failure_strain, autoclave_sti_failure_strain) % h=0, p=0.0948

```

10.17 Expense Report

Item	Description	Manufacturer	Mft Pt#	Vendor	Vendor Cat#	Date	QTY	Cost Each	Total	Link
Finger Sleeve										
Cable Ties	Velcro reusable 6 in cable ties 100 pack	VELCRO® Brand	VEL-40095-USA	Amazon	B0DYJWL6QS	11/20/2025	1	\$7.94	\$7.94	Cable Tie Link
D Ring	Connection piece between sleeve and chain	Grainger	B38R	Maker Space	N/A	11/21/2025	6	\$0.45	\$2.69	D Ring Link
Velcro Scrap	Double sided velcro strap used for prototype	VELCRO® Brand	VEL-30836-USA	Maker Space	N/A	11/20/2025	1	\$0.18	\$0.18	Velcro Tie Link
Ballistic Nylon	Fabric for the finger sleeve	Canwil Textiles	N1050D/60BK	Maker Space	N/A	11/20/2025	1	\$15.00	\$15.00	Nylon Link
Silicone Rubber	Attachable fabric to increase grip on finger	Yuhanglix	B001	Amazon	B0DFHDYDS8	11/20/2025	1	\$9.98	\$9.98	Silicone Link
Mechanical Stand										
Rubber Stopper	Secures sleeve-to-stand attachment piece, restricts unwanted rotation	NRS	77405.01	Maker Space	N/A	11/21/2025	1	\$0.15	\$0.15	Stopper Link
Medline Stand	IV stand to be rolled and clamped onto hospital bed	UISKOPW	87260610	Amazon	B0F5W8CK8X	11/20/2025	1	\$27.99	\$27.99	Stand Link
Beads	Connection method for the sleeve and stand	Tiparts	BSK8042	Amazon	B07HT1TCRR	11/20/2025	1	\$7.99	\$7.99	Bead Link
								TOTAL:	\$71.92	